american physiological society
PHYSIOLOGICAL GENOMICS

Physiol Genomics 55: 113–131, 2023.
First published January 16, 2023; doi:10.1152/physiolgenomics.00143.2022

RESEARCH ARTICLE

Comparative Physiological Genomics

Na^+/Cl^- cotransporter 2 is not fish-specific and is widely found in amphibians, non-avian reptiles, and select mammals

Toya Motoshima,[1] Ayumi Nagashima,[1] Chihiro Ota,[1] Haruka Oka,[1] Kohei Hosono,[1] Ingo Braasch,[2] Hidenori Nishihara,[1] and Akira Kato[1]

[1]*School of Life Science and Technology, Tokyo Institute of Technology, Yokohama, Japan and* [2]*Department of Integrative Biology, College of Natural Science, Michigan State University, East Lansing, Michigan, United States*

Abstract

Solute carrier 12 (Slc12) is a family of electroneutral cation-coupled chloride (Cl^-) cotransporters. $Na^+/K^+/2Cl^-$ (Nkcc) and Na^+/Cl^- cotransporters (Ncc) belong to the Nkcc/Ncc subfamily. Human and mouse possess one gene for the Na^+/Cl^- cotransporter (*ncc* gene: *slc12a3*), whereas teleost fishes possess multiple *ncc* genes, *slc12a3* (*ncc1*) and *slc12a10* (*ncc2*), in addition to their species-specific paralogs. Amphibians and squamates have two *ncc* genes: *slc12a3* (*ncc1*) and *ncc3*. However, the evolutionary relationship between *slc12a10* and *ncc3* remains unresolved, and the presence of *slc12a10* (*ncc2*) in mammals has not been clarified. Synteny and phylogenetic analyses of vertebrate genome databases showed that *ncc3* is the ortholog of *slc12a10*, and *slc12a10* is present in most ray-finned fishes, coelacanths, amphibians, reptiles, and a few mammals (e.g., platypus and horse) but pseudogenized or deleted in birds, most mammals, and some ray-finned fishes (pufferfishes). This shows that *slc12a10* is widely present among bony vertebrates and pseudogenized or deleted independently in multiple lineages. Notably, as compared with some fish that show varied *slc12a10* tissue expression profile, spotted gar, African clawed frog, red-eared slider turtle, and horse express *slc12a10* in the ovaries or premature gonads. In horse tissues, an unexpectedly large number of splicing variants for Slc12a10 have been cloned, many of which encode truncated forms of Slc12a10, suggesting that the functional constraints of horse *slc12a10* are weakened, which may be in the process of becoming a pseudogene. Our results elaborate on the evolution of Nkcc/Ncc subfamily of Slc12 in vertebrates.

NEW & NOTEWORTHY *slc12a10* is not a fish-specific gene and is present in a few mammals (e.g., platypus and horse), non-avian reptiles, amphibians, but was pseudogenized or deleted in most mammals (e.g., human, mouse, cat, cow, and rhinoceros), birds, and some ray-finned fishes (pufferfishes).

evolution; pseudogenization; Ncc2; Slc12a10; Slc12a3

INTRODUCTION

Solute carrier 12 (Slc12) is a family of electroneutral cation-coupled Cl^- cotransporters (Cccs) (protein names are not italicized, and the first letter is uppercase in this manuscript) consisting of nine members, Slc12a1–9, in human and mouse (1, 2). Slc12a1 and Slc12a2 are known as $Na^+/K^+/2Cl^-$ cotransporter 2 (Nkcc2) and Nkcc1, respectively, which mediate the electroneutral cotransport of Na^+, K^+, and $2Cl^-$. Slc12a3 is known as the Na^+/Cl^- cotransporter (Ncc), and Slc12a4–7 as K^+/Cl^- cotransporters (Kcc1–4). Nkcc2 and Ncc, which are part of the Nkcc/Ncc subfamily (3), are specifically expressed in the renal tubule of mammals and localized in the apical membrane of the thick ascending limb of Henle's loop (TAL) and distal convoluted tubule (DCT), respectively. Both Nkcc and Ncc are inhibited by the most commonly used diuretic drugs in humans, such as furosemide and thiazide diuretics, respectively (1, 2). They are responsible for the Na^+ and Cl^- reabsorption required for fluid volume and blood pressure homeostasis (4–6). Nkcc1 is ubiquitously expressed in various cells and localized in the basolateral membranes of various secretory epithelial cells secreting Cl^-. In Cl^- secretory cells, Cl^- is absorbed by Nkcc1 in the basolateral membrane and then secreted by Cl^- channels, such as cystic fibrosis transmembrane conductance regulator (Cftr) in the apical membrane (7).

The Nkcc/Ncc subfamily of Slc12 is also important for osmoregulation in fish acclimated to fresh water and seawater. Ncc or Ncc1 (Slc12a3) was initially identified as a thiazide-sensitive Na^+/Cl^- cotransporter (Tsc, also named Ncc) in the urinary bladder of winter flounder (*Pseudopleuronectes americanus*) (8). In the kidneys of freshwater teleosts, Nkcc2 and Ncc1 are expressed in the distal tubules and collecting

Correspondence: A. Kato (akirkato@bio.titech.ac.jp).
Submitted 19 September 2022 / Revised 28 December 2022 / Accepted 12 January 2023

ducts, respectively, and may be responsible for the Na^+ and Cl^- reabsorption required for hypo-osmotic urine production and net water excretion (9–11). In the gills of seawater fish, Nkcc1 is expressed in the basolateral membrane of ionocytes and supplies Cl^- into the cytoplasm for excretion by the apical Cftr Cl^- channel (12, 13). In contrast to mammals, Nkcc2 is also expressed in the fish intestine and may be responsible for intestinal Na^+ and Cl^- absorption (14–16).

A novel member of Slc12, Slc12a10 (Nccβ, Ncc2, or Ncc-like protein), was identified as a novel homolog of Ncc in euryhaline fishes by two individual groups. In 2001, the presence of two *ncc* genes (gene names are italicized, all lowercase, in this study) in the teleost European eel (*Anguilla anguilla*) was identified (17). Cutler and Cramb (2008) comprehensively characterized these two genes and named them *nccα* and *nccβ*, which were later confirmed to be *slc12a3* and *slc12a10*, respectively (14). Hiroi et al. (18) also isolated Slc12a10 by immunoscreening a cDNA expression library constructed from the gills of freshwater-acclimatized Mozambique tilapia (*Oreochromis mossambicus*). European eel Nccβ (Slc12a10), expressed in *Xenopus* oocytes, functions as an Na^+/Cl^- cotransporter with some major characteristics, making it different from Ncc1 (Slc12a3), such as being resistant to thiazide, not activated by low-chloride hypotonic stress, and exhibiting chloride currents (19, 20). In the gills of freshwater-acclimated euryhaline fish (Mozambique tilapia) and freshwater fish (zebrafish), Ncc2 (Slc12a10) is expressed in the apical membrane of ionocytes (18, 21) and is involved in branchial ion uptake from environmental water and freshwater acclimation. Ionocytes are transport epithelial cells scattered over the surface of the gills and skin of fishes and amphibians, and are responsible for maintaining body fluid ion homeostasis and osmolarity (13, 22). In freshwater teleosts and amphibians, ionocytes actively absorb salts from environmental water against the chemical gradients of ions and express ion-absorptive membrane transport proteins such as Na^+/H^+ exchanger 3 (Nhe3 or Slc9a3), Slc12a10, and epithelial Ca^{2+} channel (Ecac or Trpv6) in the apical membrane and Nka (Na^+/K^+-ATPase) in the basolateral membrane. In seawater teleosts, ionocytes actively secrete salts into the environmental water against the chemical gradients of ions and express Cftr Cl^- channels in the apical membrane and Nka and Nkcc1 in the basolateral membrane. In zebrafish embryos, knockdown of *slc12a10.2* decreased both Cl^- influx and Cl^- content (21). The transcription of *slc12a10.2* in the gills of zebrafish is upregulated by prolactin, a well-known regulator of ion and water transport in freshwater fish (23). Therefore, Slc12a10 is considered to be involved in Cl^- absorption and freshwater acclimation in fish.

Hartmann et al. (3) analyzed the evolution of the *ccc* family and showed that amphibians and squamates have two *ncc* genes, *ncc1* and *ncc3* . However, the evolutionary relationship between *ncc2* (*slc12a10*) and *ncc3* has not yet been clarified, and the presence of *ncc2/ncc3* in mammals has not been elucidated. In this study, we analyzed *slc12a10* in various vertebrate species using comparative genomic analysis of genome databases. *slc12a10* has been identified in fishes, amphibians, reptiles, monotremes, and horses, but not in birds, marsupials, and most eutherians. Tetrapod *ncc3* is an ortholog of fish *ncc2* (*slc12a10*), showing that *slc12a10* (*ncc2/ncc3*) is widely present among bony vertebrates and pseudogenized or deleted independently in multiple lineages of fish, avian, and mammalian species.

MATERIALS AND METHODS

Synteny Analysis and Identification of *slc12a10* Genes

Synteny analysis was performed with Ensembl genome browser (https://www.ensembl.org) (24) or the National Center for Biotechnology Information (NCBI) genome data viewer (https://www.ncbi.nlm.nih.gov/genome/gdv/) using genome databases of various species including human (*Homo sapiens*; GCA_000001405.29), mouse (*Mus musculus*; GCA_000001635.9), cow (*Bos taurus*; GCA_002263795.3), megabat (*Pteropus vampyrus*; GCA_000151845.2), horse (*Equus caballus*; GCA_002863925.1), platypus (*Ornithorhynchus anatinus*; GCA_004115215.4), Bengalese finch (*Lonchura striata*; GCA_005870125.1), American alligator (*Alligator mississippiensis*; GCA_000281125.4), painted turtle (*Chrysemys picta*; GCA_000241765.5), green anole (*Anolis carolinensis*; GCA_000090745.2), western clawed frog (*Xenopus tropicalis*; GCA_000004195.4), coelacanth (*Latimeria chalumnae*; GCA_000225785.1), spotted gar (*Lepisosteus oculatus*; GCA_000242695.1), Asian arowana (*Scleropages formosus*; GCA_900964775.1), zebrafish (*Danio rerio*; GCA_000002035.4), northern pike (*Esox lucius*; GCA_011004845.1), Japanese pufferfish (*Takifugu rubripes*; GCA_901000725.2), whitespotted bamboo shark (*Chiloscyllium plagiosum*; GCA_004010195.1), thorny skate (*Amblyraja radiate*; GCA_010909765.2), elephant shark (*Callorhinchus milii*; GCA_018977255.1), inshore hagfish (*Eptatretus burger*; GCA_024346535.1), and sea lamprey (*Petromyzon marinus*; GCA_010993605.1).

Phylogenetic Analysis

The amino acid sequences of Slc12a10 were obtained from genome databases of various species (Tables 1 and 2). The predicted or determined amino acid sequences of Slc12a10 were aligned using ClustalW software (25) and a phylogenetic tree was constructed using the molecular evolutionary genetics analysis (MEGA) software (26) based on the maximum-likelihood (ML) method with 100 bootstrap replicates.

Dot Plot Analysis

For comparison among intact *slc12a10* genes, the ~10 kb corresponding genomic regions of horse (*Equus caballus*), platypus (*Ornithorhynchus anatinus*), painted turtle (*Chrysemys picta*), and Western clawed frog (*Xenopus tropicalis*) were used. To compare the intact *slc12a10* gene and pseudogenes, ~10 kb corresponding genomic regions of megabat (*Pteropus vampyrus*), white rhino (*Ceratotherium simum*), cat (*Felis catus*), American black bear (*Ursus americanus*), European polecat (*Mustela putorius*), chacoan peccary (*Catagonus wagneri*), cow (*Bos taurus*), dolphin (*Tursiops truncatus*), human (*Homo sapiens*), tarsier (*Carlito syrichta*), greater bamboo lemur (*Prolemur simus*), squirrel (*Ictidomys tridecemlineatus*), Alpine marmot (*Marmota marmota*), and American beaver (*Castor canadensis*) were used. To analyze the deletion of *slc12a10* genes, ~30 kb corresponding to the genomic region of horse encoding *slc12a1* and the flanking genes (*osgep* and *klhl*) and mouse (*Mus musculus*)

Table 1. *Amino acid sequences of Slc12a10 and Slc12a3 used for the phylogenetic analysis*

Gene	Species	Accession No.
slc12a10	Horse (*Equus caballus*)	XP_023472263.1
slc12a10	Donkey (*Equus asinus*)	XP_014699999
slc12a10	Platypus (*Ornithorhynchus anatinus*)	XP_028933254
slc12a10	Red-eared slider (*Trachemys scripta*)	XP_034642584.1
slc12a10	Painted turtle (*Chrysemys picta*)	XP_023966996.1
slc12a10	American alligator (*Alligator mississippiensis*)	XP_019334996.1
slc12a10	Green anole (*Anolis carolinensis*)	XP_016850886.1
slc12a10	Two-lined caecilian (*Rhinatrema bivittatum*)	XP_029437368.1
slc12a10	African clawed frog (*Xenopus laevis*)	XP_018099460.1
slc12a10	Western clawed frog (*Xenopus tropicalis*)	XP_002934326.2
slc12a10	Coelacanth (*Coelacanthiformes*)	XP_006011463.1
slc12a10.1	Asian arowana (*Scleropages formosus*)	XP_029112028
slc12a10.2	Asian arowana (*Scleropages formosus*)	ENSSFOT00015066387.1
slc12a10.1	Zebrafish (*Danio rerio*)	XP_021333255.1
slc12a10.2	Zebrafish (*Danio rerio*)	NP_001038466.1
slc12a10.3	Zebrafish (*Danio rerio*)	XP_021333240.1
slc12a10	Northern pike (*Esox lucius*)	XP_019898755.1
slc12a10.1	Nile tilapia (*Oreochromis niloticus*)	XP_003454830.1
slc12a10.2	Nile tilapia (*Oreochromis niloticus*)	XP_019209684.1
slc12a10.3	Nile tilapia (*Oreochromis niloticus*)	XP_025761425.1
slc12a10.1	Swamp eel (*Monopterus albus*)	ENSMALT00000029818.1
slc12a10.2	Swamp eel (*Monopterus albus*)	XP_020443852.1
slc12a10.3	Swamp eel (*Monopterus albus*)	XP_020443847
slc12a10	Turbot (*Scophthalmus maximus*)	XP_035473837.1
slc12a10	Spotted gar (*Lepisosteus oculatus*)	XP_015194990.1
slc12a3	Human (*Homo sapiens*)	NP_000330.3
slc12a3	Mouse (*Mus musculus*)	XP_017168114.1
slc12a3	Cow (*Bos taurus*)	XP_015331192.1
slc12a3	Horse (*Equus caballus*)	XP_014593920.2
slc12a3	Donkey (*Equus asinus*)	XP_014682837.1
slc12a3	Koala (*Phascolarctos cinereus*)	XP_020821431.1
slc12a3	Platypus (*Ornithorhynchus anatinus*)	XP_028931599.1
slc12a3	Chicken (*Gallus domesticus*)	XP_414059.4
slc12a3	Great tit (*Parus major*)	XP_015495610.1
slc12a3	Red-eared slider (*Trachemys scripta*)	XP_034644711.1
slc12a3	Painted turtle (*Chrysemys picta*)	XP_005306320.2
slc12a3	American alligator (*Alligator mississippiensis*)	XP_014466479.1
slc12a3	Green anole (*Anolis carolinensis*)	ENSACAG00000007601
slc12a3	Two-lined caecilian (*Rhinatrema bivittatum*)	XP_029464580.1
slc12a3	African clawed frog (*Xenopus laevis*)	XP_018113335.1
slc12a3	Western clawed frog (*Xenopus tropicalis*)	XP_002937217.2
slc12a3	Coelacanth (*Coelacanthiformes*)	XP_014349758.1
slc12a3	Asian arowana (*Scleropages formosus*)	XP_018582182.2
slc12a3	Zebrafish (*Danio rerio*)	NP_001038545.1
slc12a3	Northern pike (*Esox lucius*)	XP_010882277.3
slc12a3	Nile tilapia (*Oreochromis niloticus*)	XP_003439425.1
slc12a3	Swamp eel (*Monopterus albus*)	XP_020470348.1
slc12a3	Turbot (*Scophthalmus maximus*)	XP_035497742.1
slc12a3	Spotted gar (*Lepisosteus oculatus*)	XP_015224044.1
slc12a3	Japanese pufferfish (*Takifugu rubripes*)	XP_003967138.2
slc12a3	Elephant shark (*Callorhinchus milii*)	AB769494
slc12a3	Bull shark (*Carcharhinus leucas*)	AB769491
slc12a3	Houndshark (*Triakis scyllium*)	AB769487
slc12a3	Thorny skate (*Amblyraja radiata*)	XP_032892075.1
slc12a3	Great white shark (*Carcharodon carcharias*)	XP_041047225.1
slc12a3	Smaller spotted catshark (*Scyliorhinus canicula*)	XP_038662802.1
slc12a3	Whale shark (*Rhincodon typus*)	XP_048461656.1
slc12a3	Whitespotted bamboo shark (*Chiloscyllium plagiosum*)	XP_043563470.1
slc12a3	Zebra shark (*Stegostoma fasciatum*)	XP_048402468.1
ncc	Inshore hagfish (*Eptatretus burgeri*)	ENSEBUG00000012657
ncca	Sea lamprey (*Petromyzon marinus*)	XP_032816158.1, BK014291
ncca	Sea lamprey (*Petromyzon marinus*)	XP_032816224.1
nccb	Sea lamprey (*Petromyzon marinus*)	XP_032816159.1, BK014292
nccb	Sea lamprey (*Petromyzon marinus*)	XP_032813619.1

encoding *osgep* and *klhl* were used. Dot plot comparisons were performed using EMBOSS dotmatcher program with a window size of 20 and a threshold score of 70 (https://www.ebi.ac.uk/Tools/emboss/).

Pseudogenization of *slc12a10* in Mammals

Sequences of the entire intergenic regions flanked by *klhl* and *osgep* from the horse (chr1:158825604–158840363,

Table 2. *Amino acid sequences of Slc12a1 and Slc12a2 used for the phylogenetic analysis*

Gene	Species	Accession No.
slc12a1	Human (*Homo sapiens*)	NP_000329
slc12a1	Mouse (*Mus musculus*)	NP_001073158
slc12a1	Cow (*Bos taurus*)	XP_005211957
slc12a1	Horse (*Equus caballus*)	XP_003363557
slc12a1	Donkey (*Equus asinus*)	XP_014708391
slc12a1	Koala (*Phascolarctos cinereus*)	XP_020831907
slc12a1	Platypus (*Ornithorhynchus anatinus*)	XP_028926912
slc12a1	Chicken (*Gallus domesticus*)	XP_004943856
slc12a1	Great tit (*Parus major*)	XP_015494209
slc12a1	Red-eared slider (*Trachemys scripta*)	XP_034640616.1
slc12a1	Painted turtle (*Chrysemys picta*)	XP_023957006
slc12a1	American alligator (*Alligator mississippiensis*)	XP_019333208
slc12a1	Green anole (*Anolis carolinensis*)	XP_003228048
slc12a1	Two-lined caecilian (*Rhinatrema bivittatum*)	XP_029430922
slc12a1	African clawed frog (*Xenopus laevis*)	XP_041442720.1
slc12a1	Western clawed frog (*Xenopus tropicalis*)	XP_012814934
slc12a1	Coelacanth (*Coelacanthiformes*)	XP_005998362
slc12a1	Asian arowana (*Scleropages formosus*)	XP_029112010
slc12a1	Zebrafish (*Danio rerio*)	XP_021323409
slc12a1	Northern pike (*Esox lucius*)	XP_010889602
slc12a1	Nile tilapia (*Oreochromis niloticus*)	XP_003456811
slc12a1	Swamp eel (*Monopterus albus*)	XP_020461370.1
slc12a1	Turbot (*Scophthalmus maximus*)	XP_035484268.1
slc12a1	Spotted gar (*Lepisosteus oculatus*)	XP_015198509.1
slc12a1	Japanese pufferfish (*Takifugu rubripes*)	XP_003969692
slc12a1a	Elephant shark (*Callorhinchus milii*)	AB769493
slc12a1b	Elephant shark (*Callorhinchus milii*)	ENSCMIG00000001429
slc12a1	Dogfish (*Squalus acanthias*)	AF521915.1
slc12a1	Houndshark (*Triakis scyllium*)	AB769486
slc12a1	Thorny skate (*Amblyraja radiata*)	XP_032870760.1
slc12a1	Great white shark (*Carcharodon carcharias*)	XP_041034348.1
slc12a1	Smaller spotted catshark (*Scyliorhinus canicula*)	XP_038640287.1
slc12a1	Whale shark (*Rhincodon typus*)	XP_048473103.1
slc12a1	Whitespotted bamboo shark (*Chiloscyllium plagiosum*)	XP_043536117.1
slc12a1	Zebra shark (*Stegostoma fasciatum*)	XP_048376460.1
slc12a2	Human (*Homo sapiens*)	NP_001037
slc12a2	Mouse (*Mus musculus*)	NP_033220
slc12a2	Cow (*Bos taurus*)	XP_005209144
slc12a2	Horse (*Equus caballus*)	XP_014586183
slc12a2	Donkey (*Equus asinus*)	XP_014715001
slc12a2	Koala (*Phascolarctos cinereus*)	XP_020865168
slc12a2	Chicken (*Gallus domesticus*)	XP_003643107
slc12a2	Great tit (*Parus major*)	XP_015509027
slc12a2	Red-eared slider (*Trachemys scripta*)	XP_034630792.1
slc12a2	Painted turtle (*Chrysemys picta*)	XP_005303117
slc12a2	American alligator (*Alligator mississippiensis*)	XP_006271569
slc12a2	African clawed frog (*Xenopus laevis*)	XP_004910530.1
slc12a2	Western clawed frog (*Xenopus tropicalis*)	XP_004910530
slc12a2	Two-lined caecilian (*Rhinatrema bivittatum*)	XP_029474981.1
slc12a2a	Coelacanth (*Coelacanthiformes*)	XP_006008712
slc12a2	Asian arowana (*Scleropages formosus*)	XP_018600303
slc12a2a	Zebrafish (*Danio rerio*)	NP_001002080
slc12a2a	Northern pike (*Esox lucius*)	XP_034152790
slc12a2a	Nile tilapia (*Oreochromis niloticus*)	XP_025765026
slc12a2a	Swamp eel (*Monopterus albus*)	XP_020474487.1
slc12a2a	Turbot (*Scophthalmus maximus*)	XP_035481136.1
slc12a2	Spotted gar (*Lepisosteus oculatus*)	XP_006626991.1
slc12a2a	Japanese pufferfish (*Takifugu rubripes*)	XP_003965092
slc12a2	Elephant shark (*Callorhinchus milii*)	AB769492
slc12a2	Dogfish (*Squalus acanthias*)	U05958
slc12a2	Houndshark (*Triakis scyllium*)	AB669487
slc12a2	Thorny skate (*Amblyraja radiata*)	XP_032873669.1
slc12a2	Great white shark (*Carcharodon carcharias*)	XP_041041631.1
slc12a2	Smaller spotted catshark (*Scyliorhinus canicula*)	XP_038660632.1
slc12a2	Whale shark (*Rhincodon typus*)	XP_020389481.2
slc12a2	Whitespotted bamboo shark (*Chiloscyllium plagiosum*)	XP_043574016.1
slc12a2	Zebra shark (*Stegostoma fasciatum*)	XP_048382048.1
Nkcca	Inshore hagfish (*Eptatretus burgeri*)	ENSEBUG00000013668
Nkccb	Inshore hagfish (*Eptatretus burgeri*)	ENSEBUG00000008526

Continued

Table 2.— *Continued*

Gene	Species	Accession No.
Nkcc	Sea lamprey (*Petromyzon marinus*)	MK779970.1
slc12a2b	Coelacanth (*Coelacanthiformes*)	XP_014340414.1
slc12a2b	Zebrafish (*Danio rerio*)	XP_003201788.4
slc12a2b	Northern pike (*Esox lucius*)	XP_010894315.1
slc12a2b	Nile tilapia (*Oreochromis niloticus*)	XP_003444497.1
slc12a2b	Swamp eel (*Monopterus albus*)	XP_020450787.1
slc12a2b	Turbot (*Scophthalmus maximus*)	XP_035496633.2
slc12a2b	Japanese pufferfish (*Takifugu rubripes*)	XP_003974595.1

equCab3), human (chr14:20436167–20446400, hg38), and mouse (chr14:50897495–50915384, mm10) genomes were obtained. The orthologous sequences found by the NCBI basic local alignment search tool (BLAST) search were retrieved from the genome assemblies of Przewalski's horse (*Equus przewalskii*; NW_007674891.1), zebra (*Equus quagga burchellii*; NC_060268.1), donkey (*Equus asinus*; PSZQ01003353.1), Malayan tapir (*Tapirus_indicus*; PVIE01004190.1), South American tapir (*Tapirus_terrestris*; PVID01004278.1), black rhinoceros (*Diceros bicornis minor*; JAJIAY010000041.1), Indian rhinoceros (*Rhinoceros unicornis*; JAFHKO0100000-11.1), Sumatran rhinoceros (*Dicerorhinus sumatrensis*; PEKH-010004986.1), platypus (*Ornithorhynchus anatinus*; NC_041740.1), and echidna (*Tachyglossus aculeatus*; NW_024044828.1), and those of the other 45 mammals were obtained using the Chain/Net track in the University of California Santa Cruz (UCSC) Genome Browser (27). The sequences, including horse *slc12a10* cDNA ENSECAT00000024318.2 retrieved from Ensembl, were aligned using MAFFT ver. 7.495 with the linsi option (28). The introns, UTRs, and regions unalienable to the horse ORF were removed from the alignment. The presence or absence of orthologous nucleotides for each horse ORF site was determined based on the alignment.

Analysis of dN/dS for Each Branch of the Perissodactyl Tree

The *slc12a10* gene or pseudogene sequences from Przewalski's horse, zebra, donkey, two tapirs, and four rhinoceroses were aligned using MAFFT ver. 7.495 with the linsi option (28). The sequences were used to estimate ω, the ratio of nonsynonymous to synonymous substitution rates (dN/dS). ω values were calculated using the free-ratio branch model with the codeml program in PAML ver. 4.9j (29), based on perissodactyl phylogeny (30, 31).

Animals

Juvenile spotted gar (*Lepisosteus oculatus*) were raised at Michigan State University from fertilized eggs as described previously (32, 33). Three unsexed individuals were euthanized by immersion in 0.4% tricaine methane sulfonate (MS-222; Syndel, Ferndale, WA), then tissues (gill, liver, head kidney, intestine, and premature gonad) were dissected and stored in RNA later solution (Thermo Fisher Scientific, Waltham, MA). Adult and larval African clawed frogs (*Xenopus laevis*), purchased from a local dealer, were maintained in an aquarium with tap water at 23°C with a 12-h:12-h light/dark cycle and fed commercial *Xenopus* pellets. Healthy frogs were anesthetized by immersion in MS-222 in 5 mM HEPES (pH 7.5) and then decapitated. Tissues for RNA preparation were removed with ophthalmic scissors, snap-frozen in liquid nitrogen, or quickly homogenized in Isogen (Nippon Gene, Tokyo, Japan), and then stored at −80°C.

The red-eared sliders, a kind gift from Akashi City Citizen's Life Bureau Environment Room in Japan, were kept in a 150-L tank supplied with tap water, maintained at 26°C with indirect sunlight from the windows, and fed commercial turtle pellets. Healthy turtles were anesthetized with 5% isoflurane (Mylan Seiyaku, Tokyo, Japan) for 30 min using a small-animal anesthetizer MK-A110 (Muromachi Kikai, Tokyo, Japan) and then decapitated. Tissues for RNA preparation were removed with scissors, snap-frozen in liquid nitrogen, and stored at −80°C. The animal protocols and procedures were approved by the Institutional Animal Experiment Committee of Michigan State University (spotted gar; animal use form PROTO201900309) and the Tokyo Institute of Technology (African clawed frog and red-eared slider).

Total RNAs of Tissues from Spotted Gar, African Clawed Frog, Red-Eared Slider, and Horse

Total RNAs were isolated from the liver, gill, intestine, kidney, and premature gonad of sexually immature spotted gar juveniles; the eye, pituitary, brain, heart, lung, stomach, intestine, liver, spleen, kidney, ovary, muscle, and skin of adult female African clawed frogs (120–160 g), testes of adult males (~70 g), and gill, kidney, skin, and fin of larvae (1.0–1.3 g); the eyes, lungs, colon, kidneys, skin, and ovaries of adult female red-eared sliders (~2 kg). Horse ovaries were gifted by Senko Farm Co., Ltd. (Kumamoto, Japan) and ovary tissues from a meat processing center were quickly sliced and stored in RNA later solution.

Total RNA of the red-eared slider ovary was isolated using the RNeasy Fibrous Tissue Mini Kit (Qiagen, Valencia, CA) and from other tissues using the acid guanidinium thiocyanate-phenol-chloroform extraction method with Isogen. The concentration and quality of RNA were measured based on UV absorbance at 260 and 280 nm and checked using denaturing agarose gel electrophoresis or Microchip Electrophoresis System for DNA/RNA Analysis MCE-202 MultiNA (Shimadzu, Kyoto, Japan) with an RNA reagent kit (Shimadzu). Total RNAs of the horse eye, lung, colon, kidney, and skin were purchased from Zyagen (San Diego, CA).

Semiquantitative Reverse Transcription-Polymerase Chain Reaction

First-strand complementary DNA was synthesized from 5 μg of total RNA using the SuperScript IV First-Strand Synthesis System (Thermo Fisher Scientific) with oligo(dT) primers and analyzed by RT-PCR as described previously (34). The cDNA was diluted eightfold with nuclease-free water and used as a template for PCR with gene-specific

primers (Table 3). Each reaction mixture (final volume, 12.5 μL) consisted of 0.25 μL cDNA (template), primers (individual final concentration, 0.25 μM), and 6.25 μL GoTaq Green Master Mix (2×; Promega, Madison, WI). The PCR conditions were as follows: initial denaturation at 94°C for 2 min, followed by 33 cycles of 94°C for 15 s (denaturation), 57°C for 30 s (annealing), 72°C for 1 min (extension), and a final extension at 72°C for 7 min. After amplification, 3 μL of the PCR mixture was diluted and loaded onto a Microchip Electrophoresis system for DNA/RNA Analysis MCE-202 MultiNA (Shimadzu, Kyoto, Japan) using a DNA-12000 reagent kit (Shimadzu) according to the manufacturer's instructions. Electrophoresis results were analyzed using MultiNA Viewer software (Shimadzu).

Cloning of Slc12a10 from Spotted Gar, African Clawed Frog, Red-Eared Slider, and Horse

Full-length cDNAs of Slc12a10s were isolated from the premature gonad of spotted gar, the ovary of African clawed frog and horse, and the eye of red-eared slider by RT-PCR using primers designed based on the genomic database (Table 3) and a high-fidelity DNA polymerase (KOD One PCR Master Mix, Toyobo, Osaka, Japan). cDNAs were directly sequenced or subcloned into pGEMHE (35) with In-Fusion Snap Assembly Master Mix (Takara Bio, Shiga, Japan) using gene-specific primers with 15-bp sequences that were complementary to the ends of the linearized pGEMHE (Table 3) and then sequenced. The sequences were deposited under GenBank/EMBL/DDBJ accession numbers (spotted gar Slc12a10, LC727724; African clawed frog Slc12a10, LC727723; red-eared slider Slc12a10, LC727721; and horse Slc12a10, LC727702–LC727720). Multiple sequence alignment was performed using Clustal W and ESPript (36) was used to produce graphical display of the results.

RESULTS

The "Ancient Fishes" Spotted Gar and Coelacanth Have Both *slc12a3* and *slc12a10*

We first confirmed the presence of *slc12a3* and *slc12a10* in the so-called ancient fishes spotted gar and coelacanth. Previous studies have also suggested the presence of both genes in these species (37). Synteny analysis of *slc12a3* and *slc12a10* in teleost fishes, such as zebrafish, northern pike, and Asian arowana, showed that *slc12a3* and *slc12a10* are located on different chromosomes, and are not present in the same locus (Fig. 1). Some teleost fishes have tandemly present paralogs for *slc12a10* (Fig. 1*A*). Furthermore, *slc12a3* has well-conserved neighboring genes such as *hurpud1*, *cetp*, and *mir-138* and *slc12a10* has relatively conserved neighboring genes such as *parp* and *klhl* (Fig. 1*A*). Phylogenetic analyses showed that the *slc12a10* paralogs of the Nile tilapia, swamp eel, zebrafish, and Asian arowana formed lineage-specific clades (Fig. 2).

Next, we searched the *slc12* family coding sequence around the neighboring genes in the genome databases of spotted gar and coelacanth and found a single *slc12a10* (spotted gar, ENSLOCG00000000965; coelacanth, ENSLACG00000000864) around the *parp* (Fig. 1*A*), in addition to a single *slc12a3* gene (spotted gar, ENSLOCG00000007841; coelacanth, ENSLACG00000010242) annotated around *hurpud*, *cetp*, and *mir-138* (Fig. 1*B*). Phylogenetic analyses of the deduced amino acid sequences of these genes confirmed that the annotations were correctly named (Fig. 2), confirming that spotted gar and coelacanth have both a *slc12a3* and a *slc12a10*.

Pufferfishes and Ocean Sunfish Lost *slc12a10*

Pufferfishes are known to have *slc12a3* (3) and the presence of *slc12a3* (Japanese pufferfish) was confirmed by synteny analysis, BLAST search, and phylogenetic analysis (Figs. 1*B* and 2). *slc12a3* was also found in other Tetraodontiformes species such as spotted green pufferfish (*Tetraodon nigroviridis*) and ocean sunfish (*Mola mola*). However, from those analyses, no *slc12a10* was found in the genome databases of these three Tetraodontiformes species (Fig. 1*B*) (data not shown).

Ncc Genes in Cartilaginous and Jawless Fishes

Cartilaginous fishes are known to possess *slc12a3* (38, 39). The presence of *slc12a3* in elephant shark (*Callorhinchus milii*), thorny skate (*Amblyraja radiata*), whale shark (*Rhincodon typus*), whitespotted bamboo shark (*Chiloscyllium plagiosum*), and zebra shark (*Stegostoma fasciatum*) was confirmed by synteny analyses, BLAST search, and phylogenetic analyses (Figs. 1*C* and 2). However, *slc12a10* gene was not found in the genome databases of these species (data not shown).

Lampreys have two *ncc* genes: *ncca* and *nccb* (40). Barany et al. (40) showed, via phylogenetic analyses, that Ncca occupied a basal position among the Slc12a3 and Slc12a10 clades. Furthermore, Nccb was basally positioned within the clade of Slc12a3. A BLAST search and phylogenetic analyses of sea lamprey (*Petromyzon marinus*) showed that it has two *ncca* and *nccb* genes, each (Fig. 2). A similar analysis of the inshore hagfish (*Eptatretus burgeri*) demonstrated that it possesses a single *ncc* gene (Fig. 2). Similar to the sea lamprey Ncca, the inshore hagfish Ncc occupied a basal position among the Slc12a3 and Slc12a10 clades.

A synteny analysis of *ncc* genes in inshore hagfish and sea lamprey is shown in Fig. 1*D*. In the inshore hagfish, the assembled genomic sequence containing *ncc* was short and no conserved neighboring genes were observed around *ncc*. The genomic data of the sea lamprey showed four *ncc* genes: two genes each for *ncca* and *nccb*. The two *ncca* genes were tandemly located in the region near an *nccb* gene. The other *nccb* gene was located on a different chromosome. On chromosome 25 of the sea lamprey, *pnp* was located near *nccb*, similar to *slc12a10* in other species. However, no other conserved neighboring genes were observed around *ncc* genes in chromosomes 25 and 20 of the sea lamprey.

Amphibians and Non-Avian Reptiles Possess *slc12a3* and *slc12a10*

slc12a3 is widely present in vertebrates, including amphibians and reptiles (3), and its presence in amphibians (Western clawed frog, African clawed frog, and two-lined caecilian) and non-avian reptiles (green anole, painted turtle, red-eared slider, and American alligator) was confirmed by synteny, BLAST, and phylogenetic analyses (Figs. 1*B* and 2).

Table 3. *Primers used in the present study*

Species	Gene	Accession	Remarks	Direction	Sequence (5′ to 3′)
Horse	*slc12a10*	XM_023616495	RT-PCR	Fw	ttcaggaaatatgactgacatgggt
				Rv	agcagaggtaaaagttggagatgat
			Full-length cDNA	Fw	atggcctcccagcagagagactatg (exon1), atgctccacatgtggagtgtcatcc (exon3)
				Rv	ttactggcagtacgtggtcagcaag
			In-Fusion cloning	Fw	gcagatcaattccccatggcctcccagcagagag (exon1), gcagatcaattccccatgctcca-catgtggagtgt (exon3)
				Rv	agaattcggatcccctactggcagtacgtggtca
African clawed frog	*slc12a10*	XM_018243971	RT-PCR	Fw	attgttcctgagtggcgagg
				Rv	agcctggagaattggtgacg
			Full-length cDNA	Fw	atggaatctcttgaatgttcctctg
				Rv	tcattggcagtatactgtgagggca
Red-eared slider	*slc12a10*	XM_034786693	In-Fusion cloning	Fw	gcagatcaattccccatggaatctcttgaatgttc
				Rv	agaattcggatcccctcattggcagtatactgtg
			RT-PCR	Fw	ggccaacaactaccagaccatgagcatgg
				Rv	gacgccccagcccggacacctgcat
Spotted gar	*slc12a10*	XM_015339504 ENSLOCT00000001087	Full-length cDNA	Fw	atgagggttgcggaggaggacgagg
				Rv	ctactggcagtagaaggtcagggca
			In-Fusion cloning	Fw	gcagatcaattccccatgagggttgcggag-gagg
				Rv	agaattcggatcccctcactggcagta-gaaggtca
			RT-PCR	Fw	gatccgggctttctacaccc
				Rv	agcatctctttgcggtcctc
Horse	*slc12a1*	XM_014738434	Full-length cDNA	Fw	atggggcagtgcaccacgaaatcc
				Rv	tcactggcagtagaaggtgagcaca
Horse	*slc12a2*	XM_014730697	In-Fusion cloning	Fw	gcagatcaattccccatggggcagtgcaccacga
				Rv	agaattcggatcccctcactggcagta-gaaggtga
Horse	*slc12a1*	XM_014738434	RT-PCR	Fw	tgggtatgaactagacaaacctcat
				Rv	agtagaaggccttgatcttcctttt
Horse	*slc12a2*	XM_014730697	RT-PCR	Fw	ctcgaagacaagccatgaaagaaat
				Rv	accagatggtatggaagtatctaac
Horse	*slc12a3*	XM_014738434	RT-PCR	Fw	tgggtatgaactagacaaacctcat
				Rv	agtagaaggccttgatcttcctttt
Horse	*actb*	NM_001081838	RT-PCR	Fw	atcaaggagaagctctgctatgtc
				Rv	aaggtggacaatgaggccagaat
African clawed frog	*slc12a1*	XM_018253092	RT-PCR	Fw	gtgggctgctctcatcactt
				Rv	tgggtggaggtgtactgaca
African clawed frog	*slc12a2*	NM_001122599	RT-PCR	Fw	agtgaggaggcaaaaggacg
				Rv	aattctggaccgagactgcg
African clawed frog	*slc12a3*	XM_018243971	RT-PCR	Fw	tgaggccaaatgtcctcgtc
				Rv	tttgttggttccctcgggtc
African clawed frog	*enac*	U23535	RT-PCR	Fw	tggggtgcaaggatggattc
				Rv	gtcgctgtatttcccaccca
African clawed frog	*nhe3*	XM_018267666	RT-PCR	Fw	ttttagcagtccgcgaccat
				Rv	tactcgggccctttgtgatg
African clawed frog	*atp5f1a*	NM_001087777	RT-PCR	Fw	tgttgtcagtccgtgtagcc
				Rv	ggcaatggaggttttgccag
Red-eared slider	*slc12a1*	XM_034784725	RT-PCR	Fw	tgacatacaagaagccagaggtaaa
				Rv	tttgactccatctctaaagctgtca
Red-eared slider	*slc12a2*	XM_034774901	RT-PCR	Fw	ggtatctctgtagcaggaatggaat
				Rv	attttaacttgcaagcagcagtagt
Red-eared slider	*slc12a3*	XM_034788820	RT-PCR	Fw	gtcatctctgtcgtgatcatgtttc
				Rv	tgcataagtgttttgactccacttc
Red-eared slider	*actb*	XM_034783321	RT-PCR	Fw	ccacaccttctacaatgaactcaga
				Rv	gattccatacccaagaaagatggct
Spotted gar	*slc12a3*	XM_015368558	RT-PCR	Fw	tggcgctgtcctattcagtg
				Rv	aaatggtcgtgggctgaact
Spotted gar	*actb*	XM_006637121	RT-PCR	Fw	tgccgcactggttgttgata
				Rv	gaagctgtagcctctctcgg
African clawed frog	*slc4a1*	XM_018234310	RT-PCR	Fw	tcacggatgccttaaacccc
				Rv	ctggaaacgctgagaccctt
African clawed frog	*slc4a2*	XM_018268937	RT-PCR	Fw	tgtcctacctgcagtgcttg
				Rv	gacagacaagttgcagtgcg
African clawed frog	*slc4a3*	XM_018235676	RT-PCR	Fw	aagtgtgctgagggctcttc
				Rv	ggtcagattgacactcgcca
African clawed frog	*slc26a3*	XM_018251417	RT-PCR	Fw	tgtattccgtgcccagttcc

Continued

Table 3.— *Continued*

Species	Gene	Accession	Remarks	Direction	Sequence (5′ to 3′)
African clawed frog	*slc26a4*	NM_001095539	RT-PCR	Rv	tcaaggaaagacaccgctcc
				Fw	acagcgaatgttgcctcctt
				Rv	gtctgctggtccgccataaa

The presence of *slc12a10* in coelacanth suggested that *slc12a10* is not a ray-finned fish-specific gene but widely present among vertebrate species, because it is a lobe-finned fish sharing common ancestors with tetrapods. BLAST search using the predicted amino acid sequence of coelacanth Slc12a10, followed by phylogenetic and synteny analyses, showed that amphibians (Western clawed frog, African clawed frog, and two-lined caecilian) and non-avian reptiles (green anole, painted turtle, red-eared slider, and American alligator) each have a single ortholog for *slc12a10* (Figs. 1*A* and 2). Some of these *slc12a10* genes are identical to *ncc3* previously reported (3). Hence, *ncc3* is the tetrapod ortholog of fish *ncc2*, and both *ncc2*/*ncc3* are denoted as *slc12a10* in the present study.

Birds Have *slc12a3*, but Not *slc12a10*

Birds are known to have *slc12a3* (3) and the presence of *slc12a3* (in chicken and great tit) was confirmed by synteny analysis, BLAST search, and phylogenetic analysis (Figs. 1*B* and 2). However, from those analyses, no *slc12a10* was found in the genome databases of 15 bird species such as owl parrot (*Strigops habroptilus*), Eurasian blue tit (*Cyanistes caeruleus*), wild turkey (*Meleagris gallopavo*), great spotted kiwi (*Apteryx haastii*), Indian peafowl (*Pavo cristatus*), burrowing owl (*Athene cunicularia*), zebra finch (*Taeniopygia guttata*), duck (*Anas platyrhynchos*), swan goose (*Anser cygnoides*), society finch (*Lonchura striata*), budgerigar *(Melopsittacus undulates*), African ostrich (*Struthio camelus*), ruff (*Philomachus pugnax*), chicken (*Gallus gallus*), and great tit (*Parus major*) (data not shown).

Monotremes Have Both *slc12a3* and *slc12a10*

The presence of *slc12a3* (Figs. 1*B* and 2) and *slc12a10* (Figs. 1*A* and 2) in the platypus was confirmed by synteny analysis, BLAST search, and phylogenetic analysis.

Presence of *slc12a3* and Lineage-Specific Pseudogenization and Deletion of *slc12a10* in Marsupials and Eutherians

The presence of *slc12a3* in marsupials (koala) and eutherians (human, mouse, cow, megabat, and horse) (3) was confirmed by synteny analysis (Fig. 1*B*) and BLAST search, which also showed that horses, but not marsupials and other eutherians, have *slc12a10* (Figs. 1*A* and 2). Many species (koala, elephant, cow, cat, megabat, and human) have pseudogenes that are homologous to a part of the horse *slc12a10* (Figs. 3 and 4). In this study, we use the term "pseudogene" in a broad sense, including all cases in which the gene is predicted to not encode a full-length solute carrier protein. When using "pseudogene" in a strict sense to include only cases in which it does not have any predicted function, the nonfunctionality of pseudogenes can be difficult to define (41). Therefore, in the broad sense here our term includes the possibility that pseudogenes have functions other than that of solute carrier protein-coding genes. Dot plot analysis showed that the pattern of deletion in *slc12a10* differs among mammalian lineages. In the perissodactylan white rhinoceros, no large regions were deleted in the *slc12a10* pseudogene (Figs. 3*B* and 4), but in mouse the entire region was deleted at the homologous locus (Fig. 3*G*).

To understand the history of *slc12a10* loss in mammals, the deletions of exons and the distributions of stop codons were visualized and compared among intact *slc12a10* and *slc12a10* pseudogenes in mammals (Fig. 4). In rhinoceroses, the *slc12a10* pseudogenes have a conserved stop codon in exon 6. Deletions of exons 4 and 16–22 regions in *slc12a10* pseudogenes in carnivores (cat, dog, panda, Hawaiian monk seal, and southern sea otter), exons 13–15 regions in Cetartiodactyla (dolphin, sheep, cow, pig, and alpaca), and exons 10–25 in Afrotheria (elephant, manatee, rock hyrax, and tenrec) were observed. Deletions of exons 5–9, 16–17, and 21–25 and a conserved stop codon in exon 14 were observed in *slc12a10* pseudogenes in primates (human, chimp, bonobo, gorilla, orangutan, gibbon, rhesus, crab-eating macaque, baboon, green monkey, golden snub-nosed monkey, marmoset, and squirrel monkey). These results suggest that pseudogenization of *slc12a10* occurred in the ancestral species of each lineage.

Evolution of *slc12a10* in Perissodactyla

The ratio of nonsynonymous to synonymous substitution rates ω (dN/dS) was analyzed in perissodactylan species using the *slc12a10* gene (horse and plain zebra) or pseudogene (Przewalski's horse, donkey, tapirs, and rhinoceroses) sequences, as shown in Fig. 5. The relatively low ω and dN values in branches leading to horse and zebra that retained intact *slc12a10* suggested the presence of functional constraints in these genes, whereas the relatively high values in branches leading to other species with the *slc12a10* pseudogene suggested the loss of functional constraints.

Tissue Distribution of *slc12a10* in an "Ancient Fish" (Spotted Gar), Amphibian (African Clawed Frog), Reptiles (Red-Eared Slider), and Mammal (Horse)

To confirm that the newly identified *slc12a10* genes are actually expressed in tissues, we conducted RT-PCR analyses of *slc12a10* in horse, red-eared slider, African clawed frog, and spotted gar (Fig. 6). Expression of *slc12a10* in the premature gonad, but not in the liver, gills, intestine, or head kidney of spotted gar (Fig. 6*A*) suggests that it is not expressed in the branchial ionocytes, in contrast to other freshwater teleosts that express *slc12a10* in the gills, which contains ionocytes (18, 21).

In adult African clawed frogs, *slc12a10* was specifically expressed in the ovary but not in the other tissues tested, including the skin (Fig. 6*B*), whereas in the larvae, it was

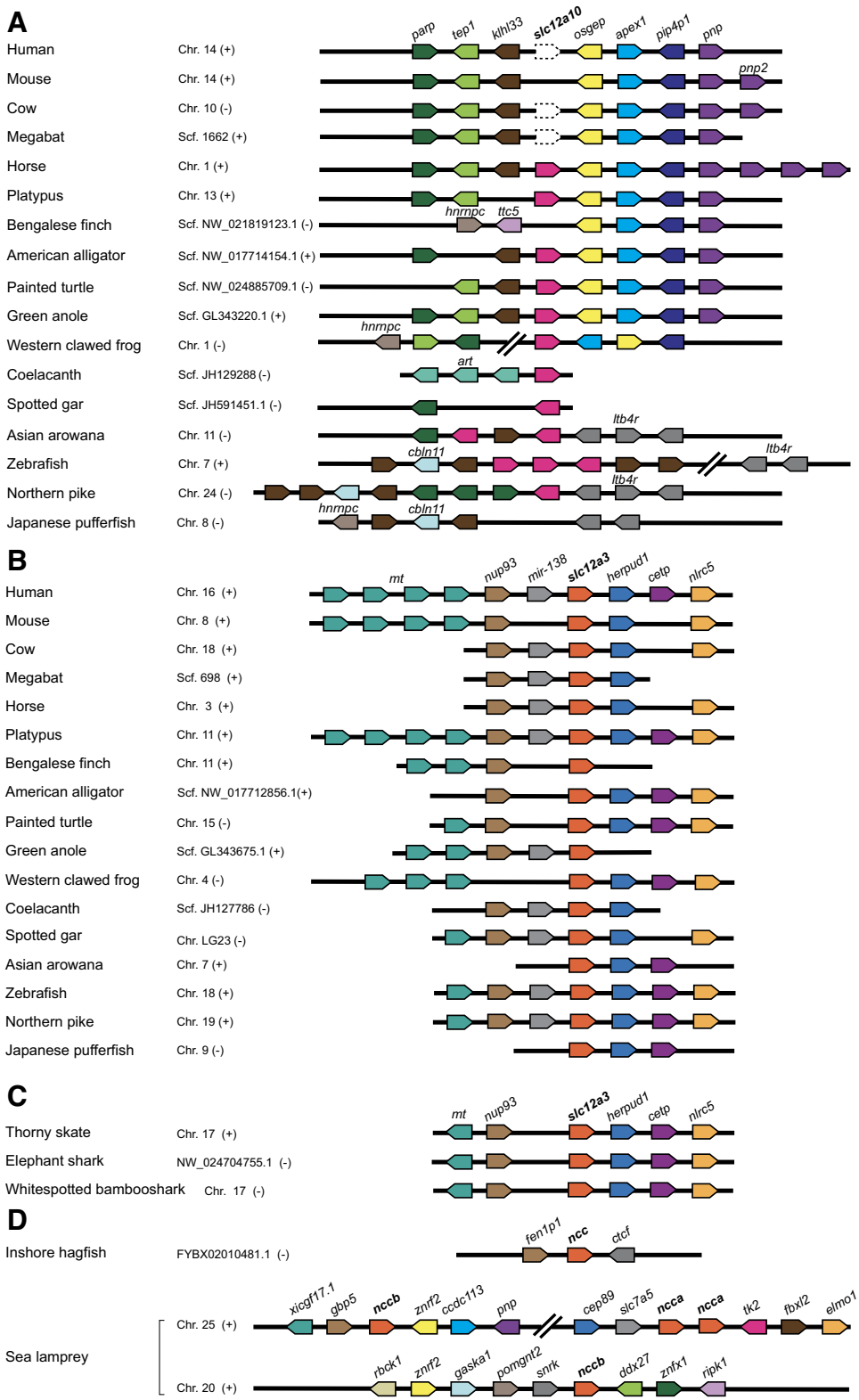

Figure 1. Synteny analyses of *slc12a10* (*A*) and *slc12a3* (*B*) in bony vertebrates, *slc12a3* in cartilaginous fishes (*C*), and *ncc* genes in jawless fishes (*D*). (+) and (−) represent the rightward and leftward orientations, respectively, of the genome sequences in NCBI and ENSEMBL databases. Arrow-shaped box indicates the orientation of each gene. Dotted arrow-shaped boxes indicate pseudogenes.

weakly expressed in the kidney but not in the gills, skin, and fin. In both adults and larvae, *slc12a1* and *slc12a3* were specifically expressed in the kidneys, whereas *slc12a2* was expressed in various tissues. In amphibians, the skin and larval gills are osmoregulatory organs that express epithelial Na^+ channels (*enac*), likely for Na^+ absorption (42, 43). The skin and larval gills of adult and larval African clawed frog expressed *enac,* but not *slc12a10*. This suggested that *slc12a10* is not involved in osmoregulation in African clawed frog.

In the red-eared slider, *slc12a10* was expressed in the ovary and also weakly in the eye, lung, and colon (Fig. 6*C*). *slc12a1*

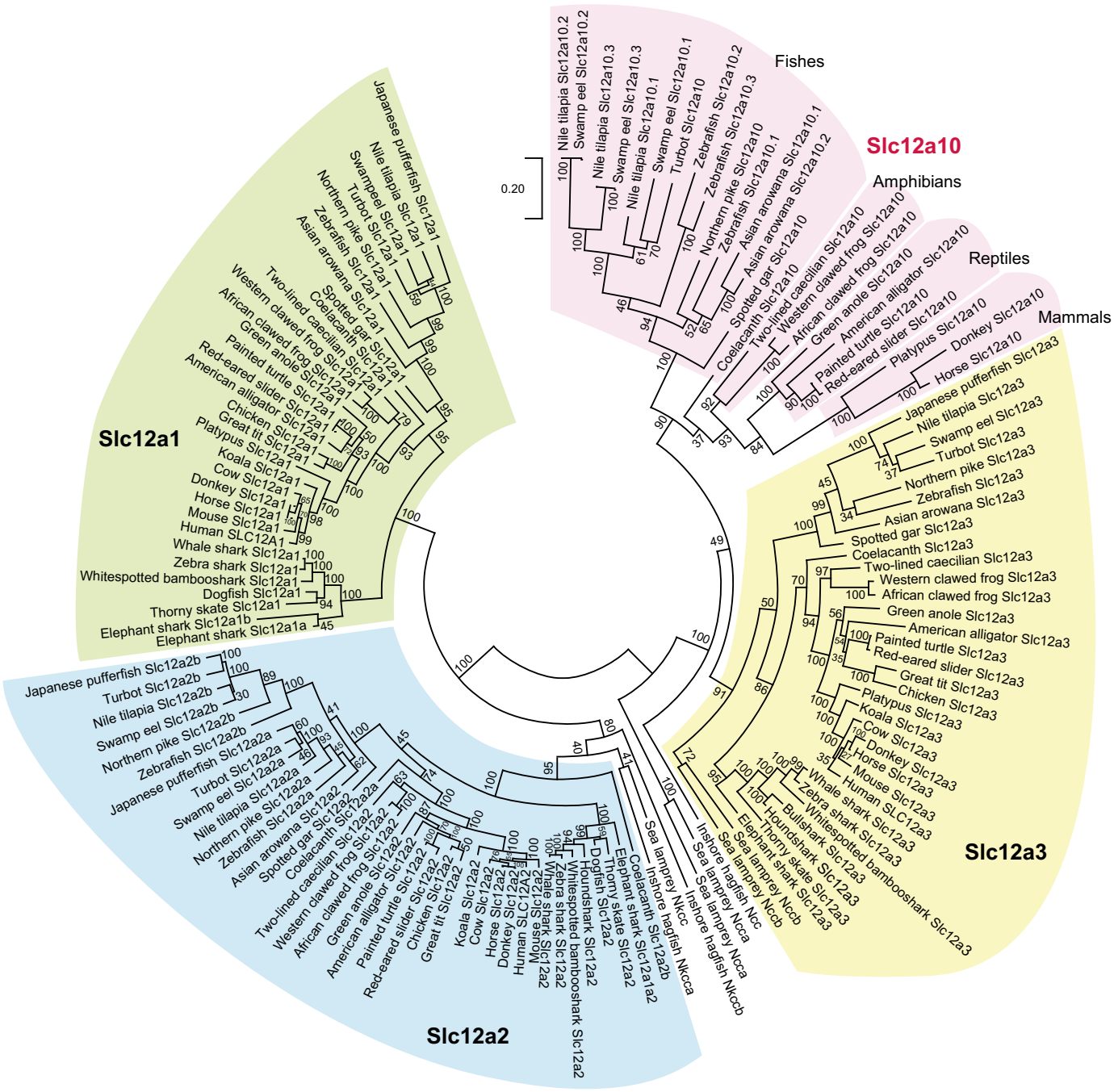

Figure 2. Phylogenetic analysis of Slc12a1, a2, a3, and a10. The amino acid sequences of Slc12a10, Slc12a1, Slc12a2, and Slc12a3 in bony vertebrates and cartilaginous fishes were aligned with Nkcc and Ncc in jawless fishes using ClustalW software and a phylogenetic tree was constructed by the maximum-likelihood method using MEGA software. Numbers indicate bootstrap values, and the scale bar represents the genetic distance of amino acid substitutions per site. The list of amino acid sequences used for the analysis is shown in Tables 1 and 2. Nkcc, $Na^+/K^+/2Cl^-$; Ncc, Na^+/Cl^- cotransporters.

and *slc12a3* were specifically expressed in the kidney, and *slc12a2* in various tissues tested. In horse, *slc12a10* was expressed in the ovary (Fig. 6*D*), *slc12a1* and *slc12a3* in the kidneys, and *slc12a2* in various tissues tested.

Cloning of cDNAs for Slc12a10 from Spotted Gar, African Clawed Frog, Red-Eared Slider, and Horse

The full-length protein-coding regions of cDNAs for Slc12a10s of spotted gar, African clawed frog, red-eared slider, and horse were cloned by RT-PCR from the total RNA isolated from the ovary or premature gonad. The multiple sequence alignment of Slc12a10s is shown in Fig. 7. Slc12a10 contains 12 putative transmembrane (TM) domains and multiple putative *N*-glycosylation sites between TM7 and 8.

The Slc12a10 of spotted gar consists of 1,041 amino acid residues and the amino acid sequences were 50%, 52%, and 58% for Slc12a1, a2, and a3, respectively, and 67%, 59%, and

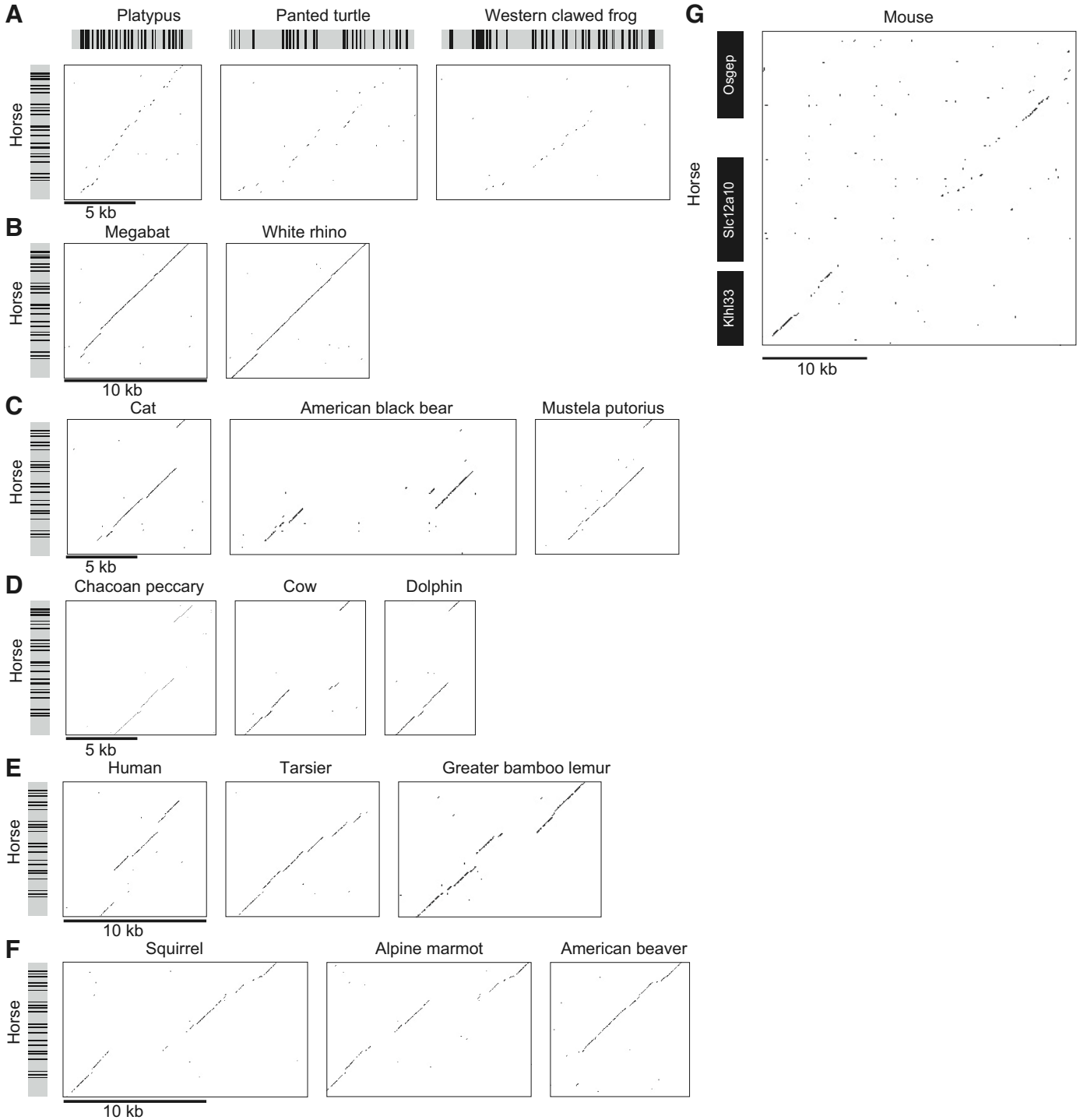

Figure 3. Dot plot analyses of the horse (*Equus caballus*) *slc12a10* gene in comparison with the corresponding genome regions of various tetrapod species. Homologous regions were plotted with dotmatcher program (window size: 20; threshold: 70). *A*: comparisons of the horse *slc12a10* gene with the *slc12a10* genes of platypus (*Ornithorhynchus anatinus*), painted turtle (*Chrysemys picta*), and Western clawed frog (*Xenopus tropicalis*). *B*: comparisons of the horse *slc12a10* gene with *slc12a10* pseudogenes of Pegasoferae species, megabat (*Pteropus vampyrus*) and white rhino (*Ceratotherium simum*). *C*: comparisons of the horse *slc12a10* gene with *slc12a10* pseudogenes of carnivores, cat (*Felis catus*), American black bear (*Ursus americanus*), and European polecat (*Mustela putorius*). *D*: comparisons of the horse *slc12a10* gene with *slc12a10* pseudogenes of cetartiodactyls, chacoan peccary (*Catagonus wagneri*), cow (*Bos taurus*), and dolphin (*Tursiops truncatus*). *E*: comparisons of the horse *slc12a10* gene with *slc12a10* pseudogenes of primates, human (*Homo sapiens*), tarsier (*Carlito syrichta*), and greater bamboo lemur (*Prolemur simus*). *F*: comparisons of the horse *slc12a10* gene with *slc12a10* pseudogenes of rodents, squirrel (*Ictidomys tridecemlineatus*), Alpine marmot (*Marmota marmota*), and American beaver (*Castor canadensis*). *G*: comparison of the *slc12a10* gene and its flanking regions with the corresponding genome region of mouse (*Mus musculus*).

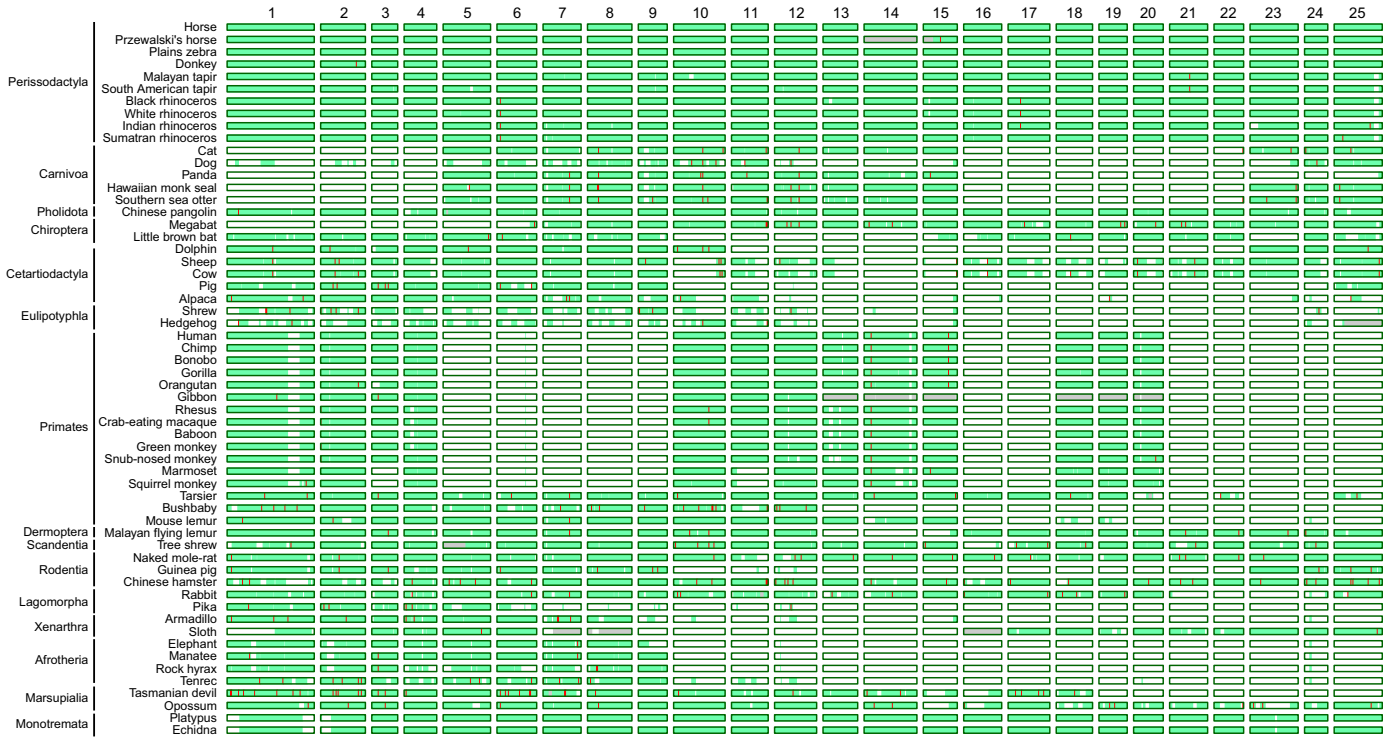

Figure 4. Deletions and nonsense mutations in the exons of *slc12a10* in mammals. The presence or absence of orthologous sequences for the horse *slc12a10* ORF, divided into 25 exons, are represented by green and white bars in each box, respectively. Undetermined regions (Ns) of the genome assemblies are shown in gray. Nonsense mutations are indicated by red bars. Order or superorder classifications of mammals are shown to the left of the species names. Lineage-specific insertions were ignored in the visualization.

61% identical to zebrafish for Slc12a10.1, a10.2, and a10.3, respectively. The African clawed frog Slc12a10 contains 1,062 amino acid residues and the amino acid sequences were 53%, 56%, and 62% for Slc12a1, a2, and a3, respectively, and 56%, 52%, and 54% identical to zebrafish for Slc12a10.1, a10.2, and a10.3, respectively. The red-eared slider Slc12a10 contains 914 amino acid residues and the amino acid sequences were 50%, 49%, and 68% for Slc12a1, a2, and a3, respectively, and 61%, 57%, and 58% identical to zebrafish for Slc12a10.1, a10.2, and a10.3, respectively. The horse Slc12a10 consists of 850 amino acid residues and the amino acid sequences were 51%, 52%, and 54% for Slc12a1, a2, and a3, respectively, and 50%, 48%, and 49% identical to zebrafish Slc12a10.1, a10.2, and a10.3, respectively.

There were very few differences in conserved sequences between Slc12a3 and Slc12a10. In Slc12a3, the-R-V-F-V-G-G- moiety was conserved in most species (Fig. 8*A*), whereas -R-V-F-I/L/V-X-X- was the corresponding site in Slc12a10 (Fig. 8*B*). In addition, the-W-W-L-F-D-D-G-G- moiety of Slc12a1 and Slc12a2 was conserved in most species (Fig. 8, *D* and *E*), whereas -Y-W-L/I/V-F/S/A-D-D-G-G- was the corresponding site in Slc12a3 and Slc12a10 (Fig. 8, *A* and *B*).

Alternative Splicing of the Horse *Slc12a10* Gene

During cloning of horse Slc12a10 cDNA from the ovarian and eye tissue, we obtained an unexpectedly large number of splicing variants, many of which did not encode full-length Slc12a10 by insertion of stop codons mainly due to frameshifts (Fig. 9). Nineteen spliced variants were isolated from the horse ovary and eye, and 16 of them encode the 3′-truncated forms of Slc12a10 by frameshifts.

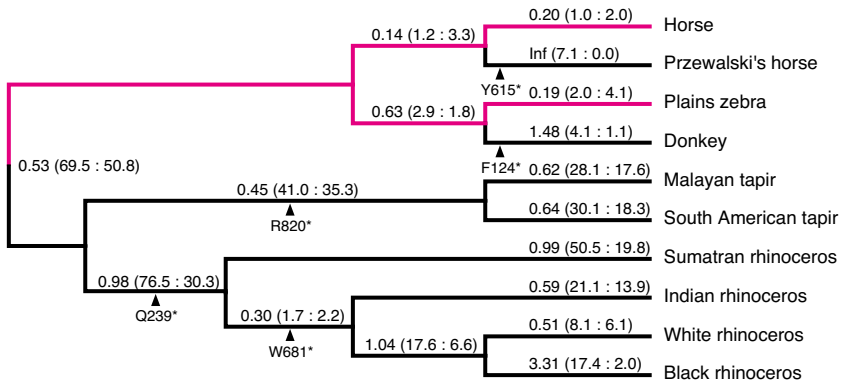

Figure 5. Pseudogenization and selective constraint of *slc12a10* in Perissodactyla. The ω (dN/dS) values and estimated numbers of nonsynonymous and synonymous substitutions (parentheses) are shown above each branch. The positions of premature stop codons due to nonsense mutations are indicated by arrowheads. Branches leading to horses and zebra that retained intact *slc12a10* are highlighted in magenta.

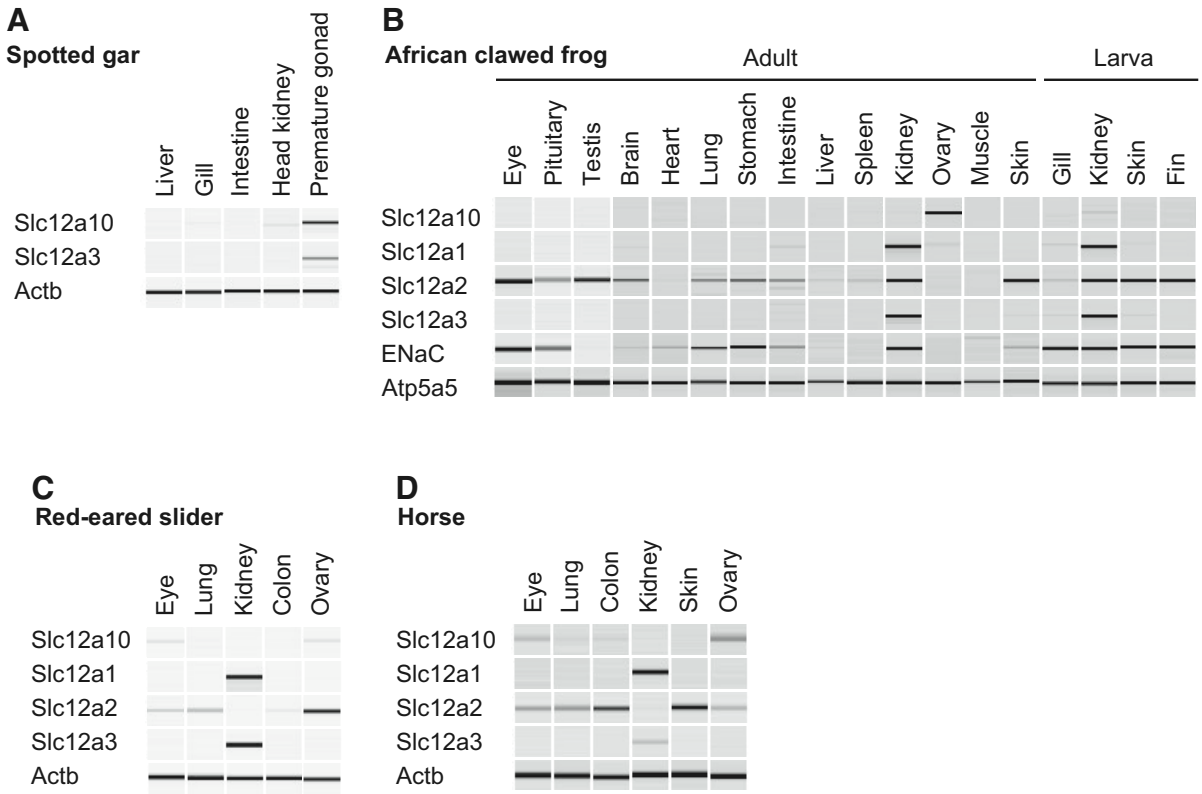

Figure 6. Tissue distribution of *slc12a10* and some related genes in spotted gar (*A*), African clawed frog (*B*), red-eared slider (*C*), and horse (*D*). *A*: expression profiles of Slc12a10 and Slc12a3 in spotted gar tissues were determined via semiquantitative RT-PCR. β-Actin (Actb) was used as an internal control. *B*: expression profiles of Slc12a10, Slc12a1, Slc12a2, Slc12a3, and Enac in African clawed frog tissues. ATP synthase F1 subunit α gene (Atp5f1a) was used as an internal control. *C*: expression profiles of Slc12a10, Slc12a1, Slc12a2, and Sc12a3 in red-eared slider tissues. β-Actin was used as an internal control. *D*: expression profiles of Slc12a10, Slc12a1, Slc12a2, and Slc12a3 in horse tissues. Actb was used as an internal control.

DISCUSSION

The present study showed that *slc12a10* is not a fish-specific gene but is widely present among bony vertebrates. Within the Slc12 family, Slc12a1, Slc12a2, Slc12a3, and Slc12a10 are closely related and form the Nkcc/Ncc subfamily. Although *slc12a1*, *slc12a2*, and *slc12a3* have been previously reported in various vertebrate species, *slc12a10* (*ncc2*) has thus far been believed to be fish-specific. Likewise, *ncc3* has been considered to be specific to amphibians and reptiles. Here, we show that fish *ncc2* and tetrapod *ncc3* are actually orthologs and clarified that *slc12a1* (*nkcc2*), *slc12a2* (*nkcc1*), *slc12a3* (*ncc* or *ncc1*), and *slc12a10* (*ncc2* or *ncc3*) are widely present among bony vertebrates.

Although *slc12a1*, *slc12a2*, and *slc12a3* were present in all tetrapods and fish species examined, *slc12a10* was deleted or pseudogenized in birds, most mammals, and some fish species. No *slc12a10* or its pseudogene was found in bird genome databases, suggesting that the loss of *slc12a10* occurred in an ancestral species of extant birds. Interestingly, within mammals, monotremes, horse, and zebra have intact *slc12a10*, and many mammalian species have *slc12a10* pseudogenes. These results suggest that pseudogenization or loss of *slc12a10* has occurred over and over again independently in numerous lineages of mammalian species. A comparison of nonsense mutations and deletions among *slc12a10* pseudogenes predicts the age of their pseudogenization. According to the mammalian evolutionary tree (Fig. 10), pseudogenization or loss of mammalian *slc12a10* occurred at least in the ancestral species of marsupial, Afrotheria, Xenarthra, Euarchontoglires, Cetartiodactyla, Chiroptera, Carnivora, Rhinocerotoidea, donkey, and Przewalski's horse, showing that gene loss or pseudogenization independently occurred in various mammalian lineages with wide phylogenetic and geographic distribution. Opossum and Tasmanian devils share nonsense mutations in exons 3 and 6, suggesting that pseudogenization occurred in their ancestors as well.

In general, pseudogenes are categorized into three groups: unprocessed duplicated, unprocessed unitary, and processed (53, 54). Unprocessed and processed pseudogenes are classified depending on whether they contain intron-derived sequences; unprocessed pseudogenes are subcategorized as duplicated and unitary depending on the presence of a functional parent gene. Dot plot analyses showed that *slc12a10* pseudogenes in mammals are unprocessed because the homologous sequences thereof were observed in both exon- and intron-coding regions. No functional parent gene was observed for *slc12a10* pseudogenes in mammals and can thus be categorized as a unitary pseudogene. Most pseudogenes lose the ability to undergo transcription; however, there are numerous examples of pseudogenes that are transcribed (53). For example, the pseudogene for the transcription factor *oct4* generates antisense RNA that combines with the sense-stranded mRNA from the parental gene to regulate expression

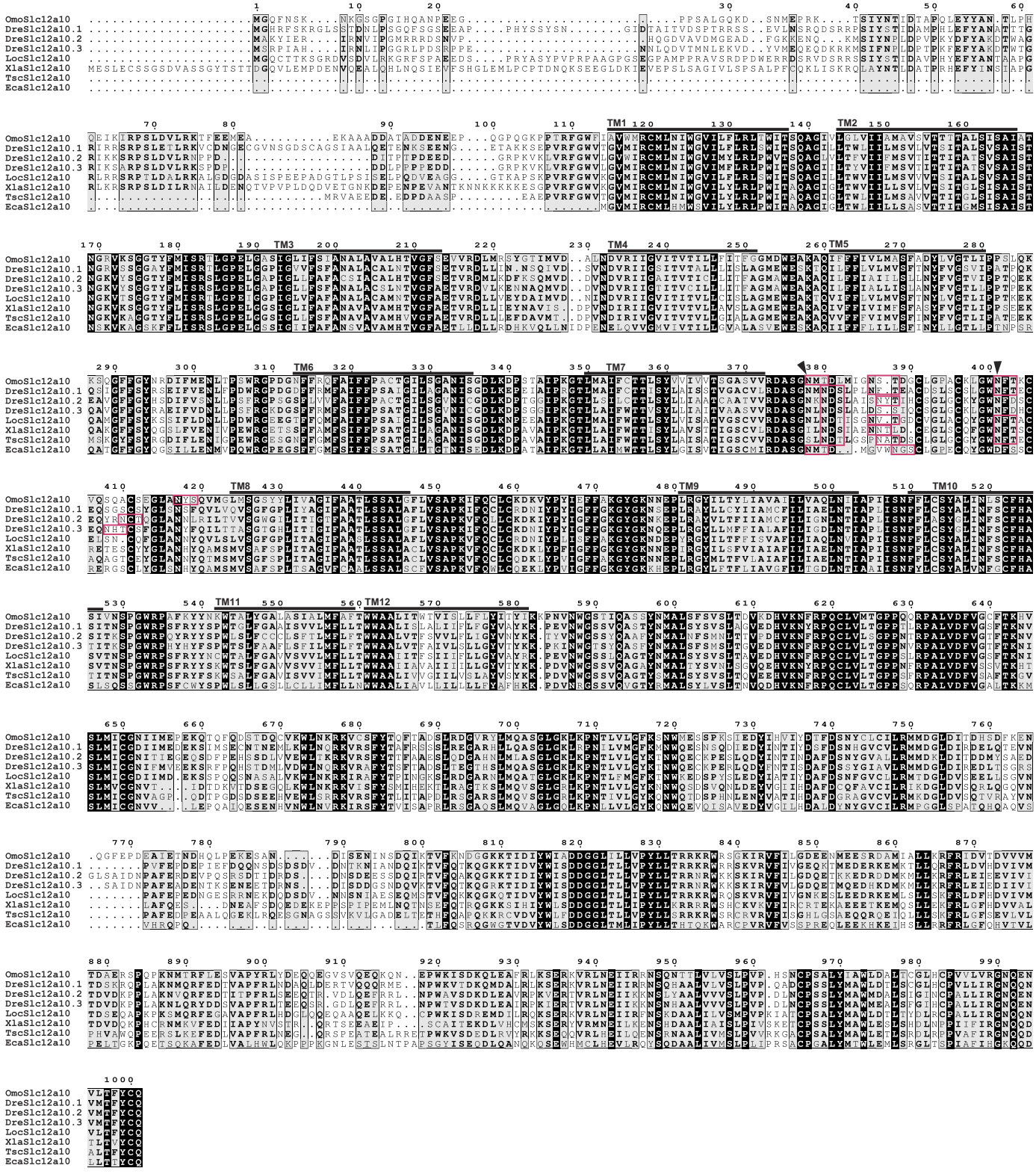

Figure 7. Multiple alignment of Slc12a10 of horse, red-eared slider, African clawed frog, spotted gar, and zebrafish. Predicted transmembrane (TM) domains are indicated by upper lines and are numbered. Putative *N*-glycosylation sites between TM7 and 8 are shown in open magenta boxes. Arrowheads indicate *N*-glycosylation sites homologous to those in mammalian Slc12a3. Conserved amino acids are shaded in black and those similar in light gray. The GenBank accession numbers are as follows: horse Slc12a10 (EcaSlc12a10), LC727702; red-eared slider Slc12a10 (TscSlc12a10), LC727721; African clawed frog Slc12a10 (XlaSlc12a10), LC727723; spotted gar Slc12a10 (LocSlc12a10), LC727724; Mozambique tilapia Slc12a10 (OmoSlc12a10), EU518934; zebrafish Slc12a10.1 (DreSlc12a10.1), NM_001161378; zebrafish Slc12a10.2 (DreSlc12a10.2), NM_001045001; and zebrafish Slc12a10.3 (DreSlc12a10.3), NM_001135131.

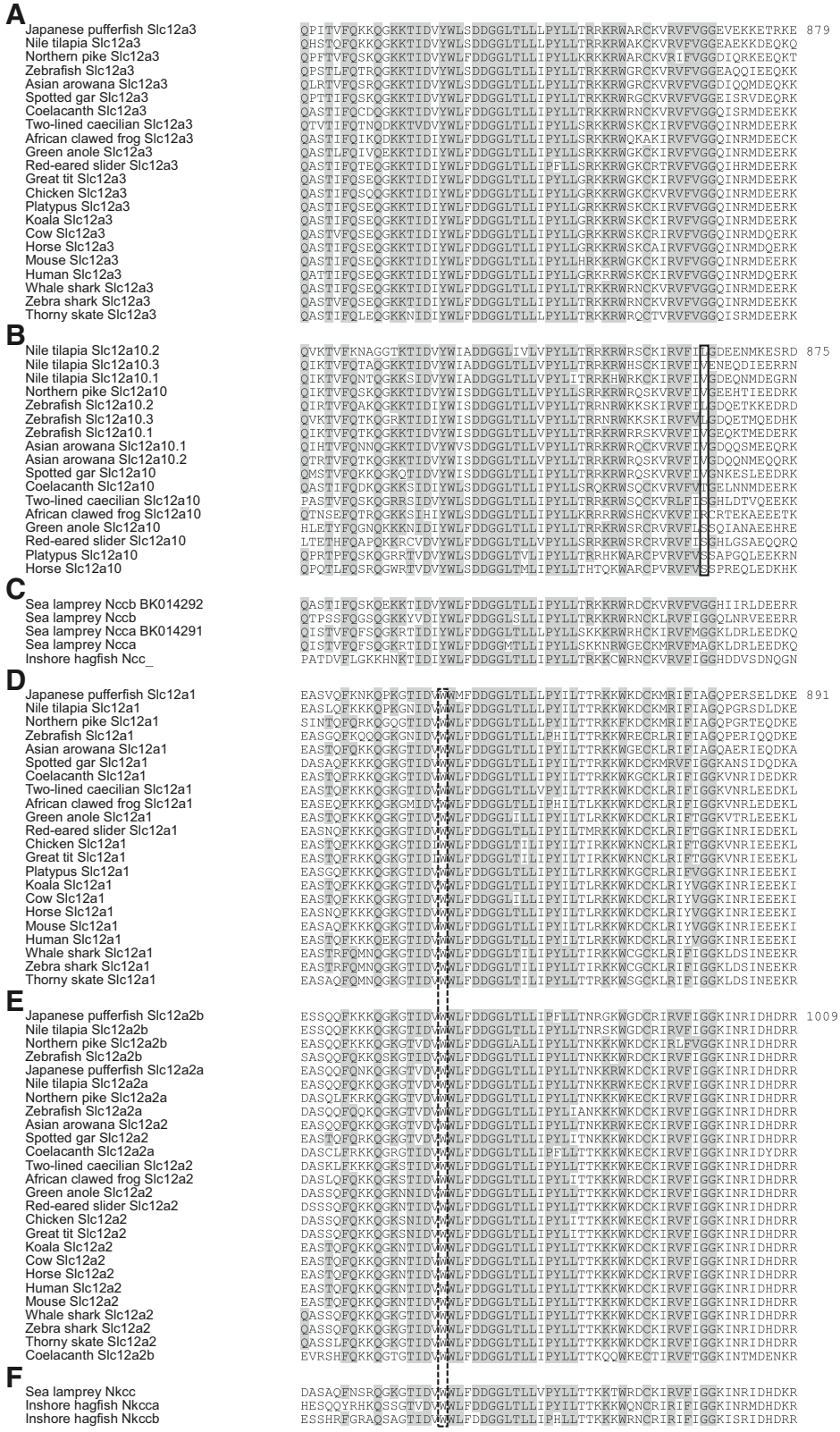

Figure 8. Conserved differences in protein sequence among Nccs and Nkccs. A portion of the aligned amino acid sequences of Slc12a3 in bony vertebrates and cartilaginous fishes (*A*), Slc12a10 in bony vertebrates (*B*), Nccs in jawless fishes (*C*), Slc12a1 in bony vertebrates and cartilaginous fishes (*D*), Slc12a2 in bony vertebrates and cartilaginous fishes (*E*), and Nkccs in jawless fishes (*F*) are depicted. *A*: conserved amino acid residues within Slc12a3 are shaded in gray. *B* and *C*: amino acid residues identical to the conserved amino acid residues of Slc12a3 are shaded in gray. The conserved difference between Slc12a3 and a10 is indicated by an open box. *D*–*F*: amino acid residues of Nkccs that are identical with the conserved amino acid residues of Slc12a3 are shaded in gray, and the conserved difference between Ncc and Nkcc is indicated by a dotted box. Amino acid residue numbers of Japanese pufferfish Slc12a3 (XP_003967138.2), Slc12a1 (XP_003969692), Slc12a2 (XP_003965092), and Nile tilapia Slc12a10.2 (XP_031596853.1) are shown to the right of the sequence. Nkcc, $Na^+/K^+/2Cl^-$; Ncc, Na^+/Cl^- cotransporters.

level (55, 56). In the case of the high mobility group A1 (*hmga1*) pseudogene, the sense-stranded RNA from this pseudogene competes for a trans-acting stability factor with mRNA for the parental gene (57). In these cases, pseudogenes regulate the function of their parent genes via their transcripts. However, in unitary pseudogenes, such mechanisms cannot be postulated because of the lack of a parent gene. To determine whether or not the *Slc12a10* pseudogene has any

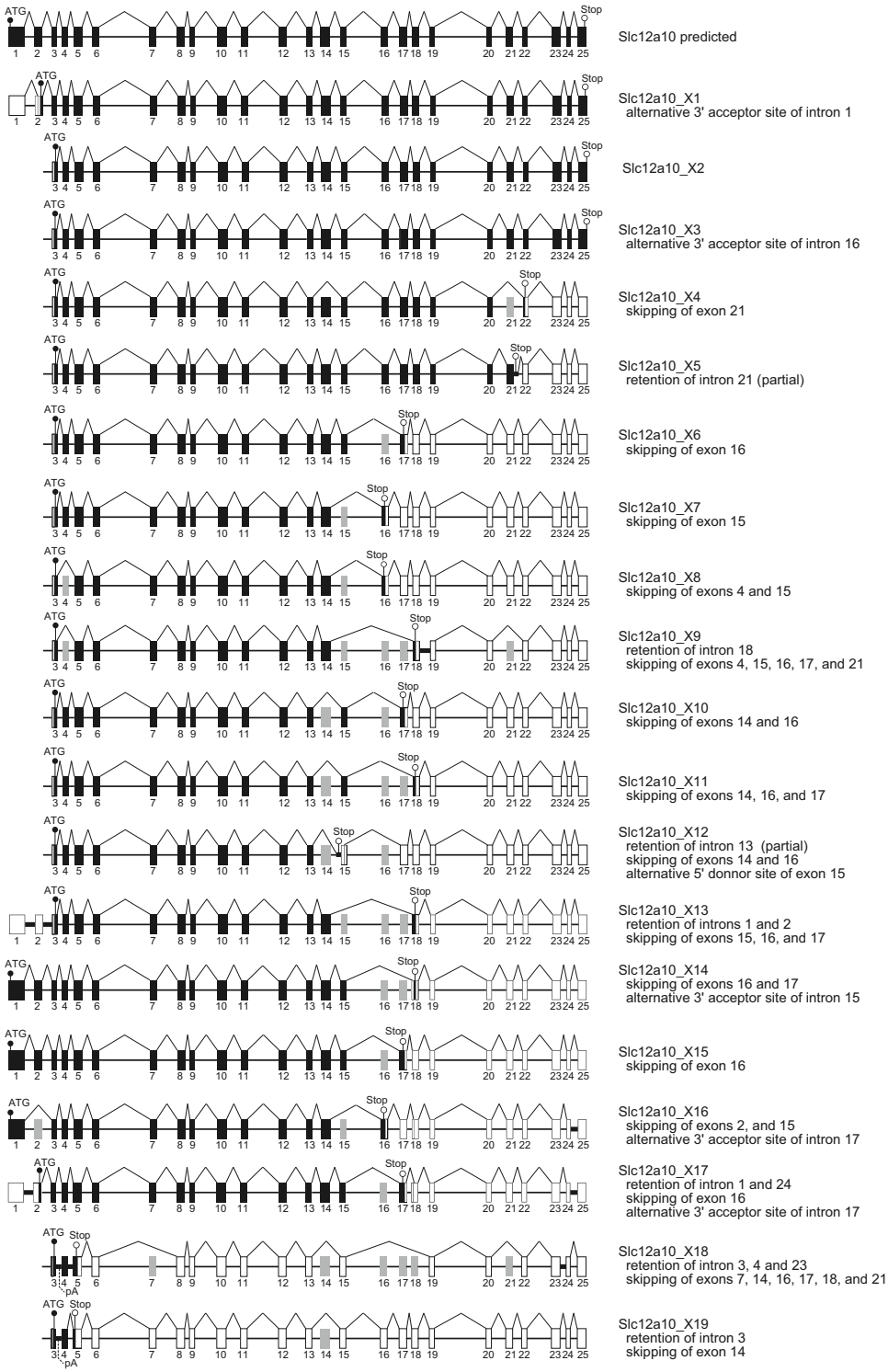

Figure 9. Alternative splicing of horse *slc12a10* gene. Diagrammatic representation of alternative splicing of horse *slc12a10* is shown. cDNA for each variant was cloned from horse tissues by RT-PCR. Exons are indicated by boxes and are numbered. The intron and flanking regions are indicated by bold lines. The coding regions of the common and alternative exons are indicated by dark and light gray boxes, respectively. Open boxes indicate UTRs. pA means predicted alternative polyadenylation sites.

function in mammals, further analysis will be required to evaluate in which species and in which organs *Slc12a10* pseudogenes may be transcribed.

Analysis of genome databases of cartilaginous and jawless fishes did not clarify the evolutionary history of the generation of Slc12a10. Previous studies (38–40) have shown that cartilaginous fishes and lampreys have *slc12a3* or *nccb* genes, respectively, and that they are located within the clade of Slc12a3 in the phylogenetic tree. The jawless fishes, lampreys and inshore hagfish, have *ncca* or *ncc* genes, which occupy a basal position among the Slc12a3 and Slc12a10 clades. No cartilaginous and jawless fish genes were positioned within the clade of Slc12a10. No clear relationship was observed between the synteny of *slc12a3* or *slc12a10* of bony vertebrates and the *ncc* genes of sea lamprey or inshore hagfish. In a previous study on the evolution of the potassium

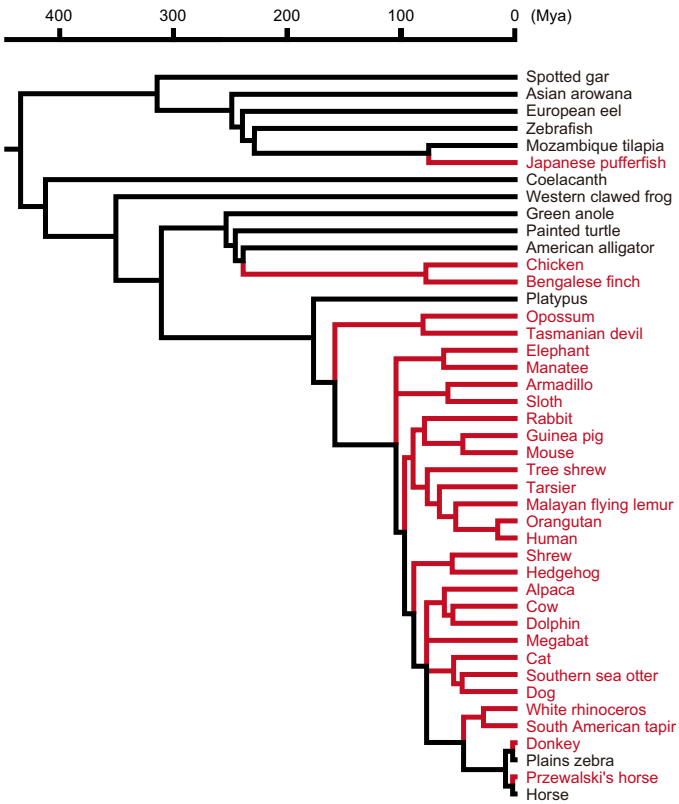

Figure 10. Evolutionary history of *slc12a10* gene in vertebrates. The phylogeny of vertebrate species with the time scale was generated based on previous studies (44–51). The names of species whose *slc12a10* are pseudogenized or deleted are shown in brown. Branches leading to species whose *slc12a10* are pseudogenized or deleted are shown as a brown line. Divergence times were retrieved from the TimeTree database (http://www.timetree.org/) (52).

voltage-gated channel *kcna* family (58), clear orthology of the sea lamprey *kcna* gene could not be established either, whereas that of the elephant shark genes to gnathostome subgroups was robustly observed. Lamprey sequences display unique codon usage patterns and amino acid compositions, which are likely associated with the exceptionally high GC content in protein-coding regions and frequently observed ambiguous molecular phylogeny of lamprey genes (58). Furthermore, as cyclostomes and gnathostomes underwent different, lineage-specific polyploidization events and thus independent duplication histories of their gene families (59, 60), pan-vertebrate orthologies from lamprey and hagfish to jawed vertebrates are notoriously difficult to establish (61). Therefore, further analysis is required to understand the evolutionary relationship of *ncc* genes between bony vertebrates and jawless fishes and to clarify the origin of *slc12a10* in bony vertebrates.

Tissue distribution analyses using RNA from multiple organs suggested an evolutionary history of the physiological function of Slc12a10. Slc12a10 was initially identified in the freshwater teleost fishes European eel and Mozambique tilapia. In Mozambique tilapia and zebrafish, Slc12a10 has been characterized as one of the apical membrane ion transporters of ionocytes in the gill, acclimatizing fishes to freshwater, and is responsible for ion uptake during osmoregulation (18, 21, 23). However, the gills of spotted gar, skin, and gills of African clawed frog adults and larvae do not express *slc12a10*. These tissues are also considered osmoregulatory sites; therefore, Slc12a10 may not be involved in ion uptake during osmoregulation in spotted gar and African clawed frog. Notably, as compared with some fish that show a variety of distributions of *slc12a10* tissue expression (14, 18, 21), *slc12a10* was expressed in the ovary/gonad of all examined species (spotted gar, African clawed frog, red-eared slider, and horse). Zebrafish have three *slc12a10* tandem paralogs: *slc12a10.1*, which is widely expressed in various tissues, including the ovary; *slc12a10.2*, which is highly expressed in the gills; and *slc12a10.3*, which is expressed in the eye and kidney (21). Therefore, the most common function of Slc12a10 in tetrapods and fishes may be related to their ovarian function, but further analysis is required to clarify its function in tissues and cells other than fish ionocytes.

The perissodactylan species horse and plain zebra have intact *slc12a10* that evolved under functional constraints, whereas Przewalski's horse, donkey, tapirs, and rhinoceroses have recently pseudogenized *slc12a10* that evolved without functional constraints after pseudogenization. In ovaries of horses, *slc12a10* was expressed, and the cloned cDNA encoding full-length Slc12a10 suggests that Slc12a10 is functional. However, we also cloned an unexpectedly large number of splicing isoforms, many of which encoded truncated forms of Slc12a10. This suggests that the functional constraints of horse *slc12a10* are weakening, and it is in the process of becoming a pseudogene. In summary, our study reveals a thus far underappreciated broad distribution of the *slc12a10* gene among bony vertebrate biodiversity that includes aquatic and terrestrial species alike.

DATA AVAILABILITY

Data will be made available upon reasonable request.

ACKNOWLEDGMENTS

We thank Yohei Sakamoto, Dr. Motoo Matsuda, and Hideo Osako for constructive discussions regarding this work; Kanji Tokushige at the Senko Farm for providing horse ovaries; Jun Tani and Hisahiro Ueda at the Natural Environment Clerk Section Environment General Affairs Division Citizens' Affairs Bureau Akashi City for providing red-eared slider; Brett Racicot for gar husbandry; and Satomi Asano, Kota Torii, Yoko Yamamoto, Nana Shinohara, the Biomaterials Analysis Division, and the Open Research Facilities for Life Science and Technology at the Tokyo Institute of Technology for technical assistance.

GRANTS

This work was supported by Japan Society for the Promotion of Science (JSPS) KAKENHI (Grant Nos. 17H03870, 21H02281, 21K14781, and 19H03272) and partially supported by the Assistant Staffing Program of the Gender Equality Section, Diversity Promotion Office, Tokyo Institute of Technology. Gar work in the Braasch Lab was supported by the US National Science Foundation EDGE Grant No. 2029216 and the R01 OD011116 Grant from the National Institutes of Health.

DISCLOSURES

No conflicts of interest, financial or otherwise, are declared by the authors.

AUTHOR CONTRIBUTIONS

T.M., A.N., and A.K. conceived and designed research; T.M., A.N., C.O., K.H., I.B., H.N., and A.K. performed experiments; T.M., A.N., C.O., H.O., K.H., H.N., and A.K. analyzed data; T.M., A.N., H.N., and A.K. interpreted results of experiments; T.M., A.N., C.O., H.N., and A.K. prepared figures; T.M., A.N., H.N., and A.K. drafted manuscript; A.N., I.B., H.N., and A.K. edited and revised manuscript; T.M., A.N., C.O., H.O., K.H., I.B., H.N., and A.K. approved final version of manuscript.

REFERENCES

1. **Arroyo JP**, **Kahle KT**, **Gamba G.** The SLC12 family of electroneutral cation-coupled chloride cotransporters. *Mol Aspects Med* 34: 288–298, 2013. doi:10.1016/j.mam.2012.05.002.
2. **Hebert SC**, **Mount DB**, **Gamba G.** Molecular physiology of cation-coupled Cl^- cotransport: the SLC12 family. *Pflugers Arch* 447: 580–593, 2004. doi:10.1007/s00424-003-1066-3.
3. **Hartmann AM**, **Tesch D**, **Nothwang HG**, **Bininda-Emonds OR.** Evolution of the cation chloride cotransporter family: ancient origins, gene losses, and subfunctionalization through duplication. *Mol Biol Evol* 31: 434–447, 2014. doi:10.1093/molbev/mst225.
4. **Bazúa-Valenti S**, **Castañeda-Bueno M**, **Gamba G.** Physiological role of SLC12 family members in the kidney. *Am J Physiol Renal Physiol* 311: F131–F144, 2016 [Erratum in *Am J Physiol Renal Physiol* 311: F830, 2016]. doi:10.1152/ajprenal.00071.2016.
5. **Castrop H**, **Schießl IM.** Physiology and pathophysiology of the renal Na-K-2Cl cotransporter (NKCC2). *Am J Physiol Renal Physiol* 307: F991–F1002, 2014. doi:10.1152/ajprenal.00432.2014.
6. **Moes AD**, **van der Lubbe N**, **Zietse R**, **Loffing J**, **Hoorn EJ.** The sodium chloride cotransporter SLC12A3: new roles in sodium, potassium, and blood pressure regulation. *Pflugers Arch* 466: 107–118, 2014. doi:10.1007/s00424-013-1407-9.
7. **Koumangoye R**, **Bastarache L**, **Delpire E.** NKCC1: newly found as a human disease-causing ion transporter. *Function (Oxf)* 2: zqaa028, 2021. doi:10.1093/function/zqaa028.
8. **Gamba G**, **Saltzberg SN**, **Lombardi M**, **Miyanoshita A**, **Lytton J**, **Hediger MA**, **Brenner BM**, **Hebert SC.** Primary structure and functional expression of a cDNA encoding the thiazide-sensitive, electroneutral sodium-chloride cotransporter. *Proc Natl Acad Sci USA* 90: 2749–2753, 1993. doi:10.1073/pnas.90.7.2749.
9. **Kato A**, **Muro T**, **Kimura Y**, **Li S**, **Islam Z**, **Ogoshi M**, **Doi H**, **Hirose S.** Differential expression of Na^+-Cl^- cotransporter and Na^+-K^+-Cl^- cotransporter 2 in the distal nephrons of euryhaline and seawater pufferfishes. *Am J Physiol Regul Integr Comp Physiol* 300: R284–R297, 2011. doi:10.1152/ajpregu.00725.2009.
10. **Teranishi K**, **Mekuchi M**, **Kaneko T.** Expression of sodium/hydrogen exchanger 3 and cation-chloride cotransporters in the kidney of Japanese eel acclimated to a wide range of salinities. *Comp Biochem Physiol A Mol Integr Physiol* 164: 333–343, 2013. doi:10.1016/j.cbpa.2012.11.011.
11. **Wingert RA**, **Selleck R**, **Yu J**, **Song HD**, **Chen Z**, **Song A**, **Zhou Y**, **Thisse B**, **Thisse C**, **McMahon AP**, **Davidson AJ.** The *cdx* genes and retinoic acid control the positioning and segmentation of the zebrafish pronephros. *PLoS Genet* 3: 1922–1938, 2007. doi:10.1371/journal.pgen.0030189.
12. **Evans DH**, **Piermarini PM**, **Choe KP.** The multifunctional fish gill: dominant site of gas exchange, osmoregulation, acid-base regulation, and excretion of nitrogenous waste. *Physiol Rev* 85: 97–177, 2005. doi:10.1152/physrev.00050.2003.
13. **Hiroi J**, **McCormick SD.** New insights into gill ionocyte and ion transporter function in euryhaline and diadromous fish. *Respir Physiol Neurobiol* 184: 257–268, 2012. doi:10.1016/j.resp.2012.07.019.
14. **Cutler CP**, **Cramb G.** Differential expression of absorptive cation-chloride-cotransporters in the intestinal and renal tissues of the European eel (*Anguilla anguilla*). *Comp Biochem Physiol B Biochem Mol Biol* 149: 63–73, 2008. doi:10.1016/j.cbpb.2007.08.007.
15. **Takei Y**, **Wong MKS**, **Ando M.** Molecular mechanisms for intestinal HCO_3^- secretion and its regulation by guanylin in seawater-acclimated eels. *J Exp Biol* 222: jeb203539, 2019. doi:10.1242/jeb.203539.
16. **Watanabe S**, **Mekuchi M**, **Ideuchi H**, **Kim YK**, **Kaneko T.** Electroneutral cation-Cl^- cotransporters NKCC2β and NCCβ expressed in the intestinal tract of Japanese eel *Anguilla japonica*. *Comp Biochem Physiol A Mol Integr Physiol* 159: 427–435, 2011. doi:10.1016/j.cbpa.2011.04.009.
17. **Cutler CP**, **Cramb G.** Molecular physiology of osmoregulation in eels and other teleosts: the role of transporter isoforms and gene duplication. *Comp Biochem Physiol A Mol Integr Physiol* 130: 551–564, 2001. doi:10.1016/s1095-6433(01)00435-4.
18. **Hiroi J**, **Yasumasu S**, **McCormick SD**, **Hwang PP**, **Kaneko T.** Evidence for an apical Na-Cl cotransporter involved in ion uptake in a teleost fish. *J Exp Biol* 211: 2584–2599, 2008. doi:10.1242/jeb.018663.
19. **Moreno E**, **Plata C**, **Rodríguez-Gama A**, **Argaiz ER**, **Vázquez N**, **Leyva-Ríos K**, **Islas L**, **Cutler C**, **Pacheco-Alvarez D**, **Mercado A**, **Cariño-Cortés R**, **Castañeda-Bueno M**, **Gamba G.** The European eel NCCβ gene encodes a thiazide-resistant Na-Cl cotransporter. *J Biol Chem* 291: 22472–22481, 2016. doi:10.1074/jbc.M116.742783.
20. **Moreno E**, **Plata C**, **Vázquez N**, **Oropeza-Viveros DM**, **Pacheco-Alvarez D**, **Rojas-Vega L**, **Olin-Sandoval V**, **Gamba G.** The European and Japanese eel NaCl cotransporters β exhibit chloride currents and are resistant to thiazide type diuretics. *Am J Physiol Cell Physiol* 323: C385–C399, 2022. doi:10.1152/ajpcell.00213.2022.
21. **Wang YF**, **Tseng YC**, **Yan JJ**, **Hiroi J**, **Hwang PP.** Role of SLC12A10.2, a Na-Cl cotransporter-like protein, in a Cl uptake mechanism in zebrafish (*Danio rerio*). *Am J Physiol Regul Integr Comp Physiol* 296: R1650–R1660, 2009. doi:10.1152/ajpregu.00119.2009.
22. **Hwang PP**, **Lee TH**, **Lin LY.** Ion regulation in fish gills: recent progress in the cellular and molecular mechanisms. *Am J Physiol Regul Integr Comp Physiol* 301: R28–R47, 2011 [Erratum in *Am J Physiol Regul Integr Comp Physiol* 301: R1206, 2011]. doi:10.1152/ajpregu.00047.2011.
23. **Breves JP**, **Serizier SB**, **Goffin V**, **McCormick SD**, **Karlstrom RO.** Prolactin regulates transcription of the ion uptake Na^+/Cl^- cotransporter (*ncc*) gene in zebrafish gill. *Mol Cell Endocrinol* 369: 98–106, 2013. doi:10.1016/j.mce.2013.01.021.
24. **Kersey PJ**, **Allen JE**, **Armean I**, **Boddu S**, **Bolt BJ**, **Carvalho-Silva D**, **Christensen M**, **Davis P**, **Falin LJ**, **Grabmueller C**, **Humphrey J**, **Kerhornou A**, **Khobova J**, **Aranganathan NK**, **Langridge N**, **Lowy E**, **McDowall MD**, **Maheswari U**, **Nuhn M**, **Ong CK**, **Overduin B**, **Paulini M**, **Pedro H**, **Perry E**, **Spudich G**, **Tapanari E**, **Walts B**, **Williams G**, **Tello-Ruiz M**, **Stein J**, **Wei S**, **Ware D**, **Bolser DM**, **Howe KL**, **Kulesha E**, **Lawson D**, **Maslen G**, **Staines DM.** Ensembl Genomes 2016: more genomes, more complexity. *Nucleic Acids Res* 44: D574–D580, 2016. doi:10.1093/nar/gkv1209.
25. **Thompson JD**, **Gibson TJ**, **Higgins DG.** Multiple sequence alignment using ClustalW and ClustalX. *Curr Protoc Bioinformatics* Chapter 2: Unit 2.3, 2002. doi:10.1002/0471250953.bi0203s00.
26. **Kumar S**, **Stecher G**, **Li M**, **Knyaz C**, **Tamura K.** MEGA X: molecular evolutionary genetics analysis across computing platforms. *Mol Biol Evol* 35: 1547–1549, 2018. doi:10.1093/molbev/msy096.
27. **Lee BT**, **Barber GP**, **Benet-Pages A**, **Casper J**, **Clawson H**, **Diekhans M**, **Fischer C**, **Gonzalez JN**, **Hinrichs AS**, **Lee CM**, **Muthuraman P**, **Nassar LR**, **Nguy B**, **Pereira T**, **Perez G**, **Raney BJ**, **Rosenbloom KR**, **Schmelter D**, **Speir ML**, **Wick BD**, **Zweig AS**, **Haussler D**, **Kuhn RM**, **Haeussler M**, **Kent WJ.** The UCSC Genome Browser database: 2022 update. *Nucleic Acids Res* 50: D1115–D1122, 2022. doi:10.1093/nar/gkab959.
28. **Katoh K**, **Standley DM.** MAFFT multiple sequence alignment software version 7: improvements in performance and usability. *Mol Biol Evol* 30: 772–780, 2013. doi:10.1093/molbev/mst010.
29. **Yang Z.** PAML 4: phylogenetic analysis by maximum likelihood. *Mol Biol Evol* 24: 1586–1591, 2007. doi:10.1093/molbev/msm088.
30. **Margaryan A**, **Lawson DJ**, **Sikora M**, **Racimo F**, **Rasmussen S**, **Moltke I et al.** Population genomics of the Viking world. *Nature* 585: 390–396, 2020 [Erratum in *Nature* 591: E29, 2021]. doi:10.1038/s41586-020-2688-8.
31. **Meredith RW**, **Janečka JE**, **Gatesy J**, **Ryder OA**, **Fisher CA**, **Teeling EC**, **Goodbla A**, **Eizirik E**, **Simão TL**, **Stadler T**, **Rabosky DL**, **Honeycutt RL**, **Flynn JJ**, **Ingram CM**, **Steiner C**, **Williams TL**, **Robinson TJ**, **Burk-Herrick A**, **Westerman M**, **Ayoub NA**, **Springer MS**, **Murphy WJ.** Impacts of the cretaceous terrestrial revolution and KPg extinction on mammal diversification. *Science* 334: 521–524, 2011. doi:10.1126/science.1211028.

32. **Braasch I**, **Guiguen Y**, **Loker R**, **Letaw JH**, **Ferrara A**, **Bobe J**, **Postlethwait JH.** Connectivity of vertebrate genomes: *Paired-related homeobox* (*Prrx*) genes in spotted gar, basal teleosts, and tetrapods. *Comp Biochem Physiol C Toxicol Pharmacol* 163: 24–36, 2014. doi:10.1016/j.cbpc.2014.01.005.
33. **Darnet S**, **Dragalzew AC**, **Amaral DB**, **Sousa JF**, **Thompson AW**, **Cass AN**, **Lorena J**, **Pires ES**, **Costa CM**, **Sousa MP**, **Fröbisch NB**, **Oliveira G**, **Schneider PN**, **Davis MC**, **Braasch I**, **Schneider I.** Deep evolutionary origin of limb and fin regeneration. *Proc Natl Acad Sci USA* 116: 15106–15115, 2019. doi:10.1073/pnas.1900475116.
34. **Tran YH**, **Xu Z**, **Kato A**, **Mistry AC**, **Goya Y**, **Taira M**, **Brandt SJ**, **Hirose S.** Spliced isoforms of LIM-domain-binding protein (CLIM/NLI/Ldb) lacking the LIM-interaction domain. *J Biochem* 140: 105–119, 2006. doi:10.1093/jb/mvj134.
35. **Liman ER**, **Tytgat J**, **Hess P.** Subunit stoichiometry of a mammalian K^+ channel determined by construction of multimeric cDNAs. *Neuron* 9: 861–871, 1992. doi:10.1016/0896-6273(92)90239-a.
36. **Robert X**, **Gouet P.** Deciphering key features in protein structures with the new ENDscript server. *Nucleic Acids Res* 42: W320–W324, 2014. doi:10.1093/nar/gku316.
37. **Takei Y**, **Hiroi J**, **Takahashi H**, **Sakamoto T.** Diverse mechanisms for body fluid regulation in teleost fishes. *Am J Physiol Regul Integr Comp Physiol* 307: R778–R792, 2014. doi:10.1152/ajpregu.00104.2014.
38. **Imaseki I**, **Wakabayashi M**, **Hara Y**, **Watanabe T**, **Takabe S**, **Kakumura K**, **Honda Y**, **Ueda K**, **Murakumo K**, **Matsumoto R**, **Matsumoto Y**, **Nakamura M**, **Takagi W**, **Kuraku S**, **Hyodo S.** Comprehensive analysis of genes contributing to euryhalinity in the bull shark, Carcharhinus leucas; Na^+-Cl^- co-transporter is one of the key renal factors upregulated in acclimation to low-salinity environment. *J Exp Biol* 222: jeb201780, 2019. doi:10.1242/jeb.201780.
39. **Takabe S**, **Inokuchi M**, **Yamaguchi Y**, **Hyodo S.** Distribution and dynamics of branchial ionocytes in houndshark reared in full-strength and diluted seawater environments. *Comp Biochem Physiol A Mol Integr Physiol* 198: 22–32, 2016. doi:10.1016/j.cbpa.2016.03.019.
40. **Barany A**, **Shaughnessy CA**, **Pelis RM**, **Fuentes J**, **Mancera JM**, **McCormick SD.** Tissue and salinity specific Na^+/Cl^- cotransporter (NCC) orthologues involved in the adaptive osmoregulation of sea lamprey (*Petromyzon marinus*). *Sci Rep* 11: 22698, 2021. doi:10.1038/s41598-021-02125-1.
41. **Tutar Y.** Pseudogenes. *Comp Funct Genomics* 2012: 424526, 2012. doi:10.1155/2012/424526.
42. **Larsen EH.** Dual skin functions in amphibian osmoregulation. *Comp Biochem Physiol A Mol Integr Physiol* 253: 110869, 2021. doi:10.1016/j.cbpa.2020.110869.
43. **Uchiyama M**, **Kumano T**, **Komiyama M**, **Yoshizawa H**, **Matsuda K.** Immunohistological classification of ionocytes in the external gills of larval Japanese black salamander, Hynobius nigrescens Stejneger. *J Morphol* 272: 1017–1024, 2011. doi:10.1002/jmor.10977.
44. **Kumar S**, **Hedges SB.** A molecular timescale for vertebrate evolution. *Nature* 392: 917–920, 1998. doi:10.1038/31927.
45. **Hasegawa M**, **Thorne JL**, **Kishino H.** Time scale of eutherian evolution estimated without assuming a constant rate of molecular evolution. *Genes Genet Syst* 78: 267–283, 2003. doi:10.1266/ggs.78.267.
46. **Nishihara H**, **Hasegawa M**, **Okada N.** Pegasoferae, an unexpected mammalian clade revealed by tracking ancient retroposon insertions. *Proc Natl Acad Sci USA* 103: 9929–9934, 2006. doi:10.1073/pnas.0603797103.
47. **Hallström BM**, **Janke A.** Resolution among major placental mammal interordinal relationships with genome data imply that speciation influenced their earliest radiations. *BMC Evol Biol* 8: 162, 2008. doi:10.1186/1471-2148-8-162.
48. **Lestari B**, **Naito S**, **Endo A**, **Nishihara H**, **Kato A**, **Watanabe E**, **Denda K**, **Komada M**, **Fukushima T.** Placental mammals acquired functional sequences in NRK for regulating the CK2-PTEN-AKT pathway and placental cell proliferation. *Mol Biol Evol* 39: msab371, 2022. doi:10.1093/molbev/msab371.
49. **Chiari Y**, **Cahais V**, **Galtier N**, **Delsuc F.** Phylogenomic analyses support the position of turtles as the sister group of birds and crocodiles (Archosauria). *BMC Biol* 10: 65, 2012. doi:10.1186/1741-7007-10-65.
50. **Hughes LC**, **Ortí G**, **Huang Y**, **Sun Y**, **Baldwin CC**, **Thompson AW**, **Arcila D**, **Betancur RR**, **Li C**, **Becker L**, **Bellora N**, **Zhao X**, **Li X**, **Wang M**, **Fang C**, **Xie B**, **Zhou Z**, **Huang H**, **Chen S**, **Venkatesh B**, **Shi Q.** Comprehensive phylogeny of ray-finned fishes (Actinopterygii) based on transcriptomic and genomic data. *Proc Natl Acad Sci USA* 115: 6249–6254, 2018. doi:10.1073/pnas.1719358115.
51. **Delsuc F**, **Kuch M**, **Gibb GC**, **Hughes J**, **Szpak P**, **Southon J**, **Enk J**, **Duggan AT**, **Poinar HN.** Resolving the phylogenetic position of Darwin's extinct ground sloth (*Mylodon darwinii*) using mitogenomic and nuclear exon data. *Proc Biol Sci* 285: 20180214, 2018. doi:10.1098/rspb.2018.0214.
52. **Kumar S**, **Stecher G**, **Suleski M**, **Hedges SB.** TimeTree: a resource for timelines, timetrees, and divergence times. *Mol Biol Evol* 34: 1812–1819, 2017. doi:10.1093/molbev/msx116.
53. **Pink RC**, **Wicks K**, **Caley DP**, **Punch EK**, **Jacobs L**, **Carter DR.** Pseudogenes: pseudo-functional or key regulators in health and disease? *RNA* 17: 792–798, 2011. doi:10.1261/rna.2658311.
54. **Zhang ZD**, **Frankish A**, **Hunt T**, **Harrow J**, **Gerstein M.** Identification and analysis of unitary pseudogenes: historic and contemporary gene losses in humans and other primates. *Genome Biol* 11: R26, 2010. doi:10.1186/gb-2010-11-3-r26.
55. **Lin H**, **Shabbir A**, **Molnar M**, **Lee T.** Stem cell regulatory function mediated by expression of a novel mouse Oct4 pseudogene. *Biochem Biophys Res Commun* 355: 111–116, 2007. doi:10.1016/j.bbrc.2007.01.106.
56. **Scarola M**, **Comisso E**, **Pascolo R**, **Chiaradia R**, **Marion RM**, **Schneider C**, **Blasco MA**, **Schoeftner S**, **Benetti R.** Epigenetic silencing of Oct4 by a complex containing SUV39H1 and Oct4 pseudogene lncRNA. *Nat Commun* 6: 7631, 2015. doi:10.1038/ncomms8631.
57. **Chiefari E**, **Iiritano S**, **Paonessa F**, **Le Pera I**, **Arcidiacono B**, **Filocamo M**, **Foti D**, **Liebhaber SA**, **Brunetti A.** Pseudogene-mediated posttranscriptional silencing of HMGA1 can result in insulin resistance and type 2 diabetes. *Nat Commun* 1: 40, 2010. doi:10.1038/ncomms1040.
58. **Qiu H**, **Hildebrand F**, **Kuraku S**, **Meyer A.** Unresolved orthology and peculiar coding sequence properties of lamprey genes: the *KCNA* gene family as test case. *BMC Genomics* 12: 325, 2011. doi:10.1186/1471-2164-12-325.
59. **Simakov O**, **Marlétaz F**, **Yue JX**, **O'Connell B**, **Jenkins J**, **Brandt A**, **Calef R**, **Tung CH**, **Huang TK**, **Schmutz J**, **Satoh N**, **Yu JK**, **Putnam NH**, **Green RE**, **Rokhsar DS.** Deeply conserved synteny resolves early events in vertebrate evolution. *Nat Ecol Evol* 4: 820–830, 2020. doi:10.1038/s41559-020-1156-z.
60. **Nakatani Y**, **Shingate P**, **Ravi V**, **Pillai NE**, **Prasad A**, **McLysaght A**, **Venkatesh B.** Reconstruction of proto-vertebrate, proto-cyclostome and proto-gnathostome genomes provides new insights into early vertebrate evolution. *Nat Commun* 12: 4489, 2021 [Erratum in *Nat Commun* 12: 4704, 2021]. doi:10.1038/s41467-021-24573-z.
61. **Kuraku S.** Impact of asymmetric gene repertoire between cyclostomes and gnathostomes. *Semin Cell Dev Biol* 24: 119–127, 2013. doi:10.1016/j.semcdb.2012.12.009.